

The Pennsylvania State University

The Graduate School

John and Willie Leone Family Department of Energy and Mineral Engineering

**SIMULATION AND OPTIMIZATION OF NATURAL GAS TRANSPORTATION  
IN PIPELINE NETWORKS USING A LINEARIZED MODEL**

A Thesis in

Energy and Mineral Engineering

by

Romulo Rodrigues de Carvalho

© 2016 Romulo Rodrigues de Carvalho

Submitted in Partial Fulfillment

of the Requirements

for the Degree of

Master of Science

May 2016

The thesis of Romulo Rodrigues de Carvalho was reviewed and approved\* by the following:

Luis F. Ayala H.

Professor of Petroleum and Natural Gas Engineering

Thesis Advisor

Turgay Ertekin

Head of the John and Willie Leone Family Department of Energy and Mineral Engineering

Professor of Petroleum and Natural Gas Engineering

Hamid Emami-Meybodi

Assistant Professor of Petroleum and Natural Gas Engineering

\*Signatures are on file in the Graduate School

## ABSTRACT

When pipelines are used to transport gas through long distances, compression stations are coupled to the system in order to regain energy that is lost during fluid flow. In order for the compression stations to work, they consume part of the fluid being transported, making of it a source of fuel. An elegant optimization problem arises from the determination of network characteristics that will minimize fuel consumption at the compression stations. This minimization problem is given by highly non-linear objective function and constraints. Furthermore, an important part of the determination of compression performance is based on the calculation of efficiency in compressors. While some authors have assumed this efficiency to be constant, others have expanded the efficiency calculations by using polynomial curves. This study introduces three methods that allow for the simulation and optimization of natural gas transportation networks: first, it is demonstrated how fuel consumption can be accounted for in a system; second, it is introduced a method for the calculation of compressor efficiency; third, a domain-constrained search procedure is implemented in order to determine how compression stations should be adjusted in order to achieve minimum fuel consumption in a given transportation network. In order to account for possible convergence difficulties, all the procedures implemented in the three methods rely on the use of the Linear-Pressure Analog model, a technique that allows for the linearization of the gas flow equations. This is concluded to be one of the main reasons why system efficiency and minimum fuel consumption can be estimated, given the fact that the Linear Analog procedure facilitates

convergence and effectiveness of the methods implemented in a reliable and effective manner.

## TABLE OF CONTENTS

LIST OF FIGURES .....	vii
LIST OF TABLES .....	ix
LIST OF SYMBOLS .....	x
ACKNOWLEDGEMENTS .....	xii
CHAPTER 1 .....	1
INTRODUCTION .....	1
CHAPTER 2 .....	5
LITERATURE REVIEW .....	5
2.1 The Gas Generalized Pipe Flow Equation Derivation .....	7
2.2 The Generalized Gas Flow Equation in $\Delta P$ -explicit form .....	16
2.3 Friction Factors .....	17
2.3.1 Colebrook Formula .....	19
2.4 Gas Network Analysis .....	20
2.4.1 The Nodal-loop Formulation or Q-formulation .....	21
2.4.2 The Nodal Formulation or P-formulation .....	22
2.5 Solution Procedures .....	23
2.5.1 The Newton-Raphson Method .....	23
2.5.2 The Linear Analog Method .....	24
CHAPTER 3 .....	29
THE COMPRESSOR .....	29
3.1 Coupling of Compressor to the System .....	33
3.2 The Compressor Efficiency .....	34
3.3 The Compressor Domain .....	37
CHAPTER 4 .....	39
THE COST MINIMIZATION MODEL .....	39
4.1 The Fuel Cost Minimization Problem .....	39
CHAPTER 5 .....	43
METHODOLOGY .....	43

5.1 Fuel Cost Function .....	44
5.2 The Estimation of Fuel Consumption .....	46
5.3 The Calculation of Compressor Efficiency.....	47
5.4 The Domain-Constrained Search Procedure.....	47
CHAPTER 6 .....	51
RESULTS AND DISCUSSION .....	51
6.1 Case Study 1 .....	51
6.2 Case Study 2 .....	57
6.3 Case Study 3 .....	66
6.3.1 Case Study 3.a: only fixed pressures at nodes 1 and 6 .....	69
6.3.2 Case Study 3.b: pressure in node 10 is constrained to be higher than 850 psi. ....	70
6.3.3 Case Study 3.c, pressure in node 10 is constrained to be higher than 880 psia. ....	71
6.3.4 Case Study 3.d, pressure in node 10 is constrained to be higher than 900 psi. ....	72
6.3.5 Case Study 3.e: constraints in pressure delivery, Surge and Stonewall conditions. .	73
6.3.6 Case Study 3.f: constraints in pressure delivery, Surge and Stonewall conditions. .	74
CHAPTER 7 .....	78
CONCLUDING REMARKS.....	78
7.1 Future Work .....	79
BIBLIOGRAPHY .....	81

## LIST OF FIGURES

Figure 1: U.S. natural gas pipeline networks. ....	2
Figure 2: Scheme of flow going through the two nodes of a pipeline. ....	5
Figure 3: Scheme of flow going through the two nodes of an inclined pipeline. ....	6
Figure 4: Trigonometric behavior of inclined pipes .....	12
Figure 5: Derivation of the Linear-Analog conductivity.. ....	26
Figure 6: The Linear-Pressure Analog algorithm.. ....	27
Figure 7: Radial-flow horizontally split multistage centrifugal compressor. ....	30
Figure 8: Scheme of a compressor coupled to a Natural Gas Transportation Network ...	31
Figure 9: Centrifugal gas compressor. ....	31
Figure 10: A compression station in Tapinhoa, Brazil. ....	32
Figure 11: Compressor domain restricted to “surge” and “stonewall” conditions. ....	38
Figure 12: General function algorithm. ....	45
Figure 13: The domain-constrained search procedure.....	48
Figure 14: Case Study 1, based on Leong and Ayala (2013).....	52
Figure 15: Linear analog characteristic matrix for Case Study 1. ....	54
Figure 16: Pressure convergence for Case Study 1. ....	55
Figure 17: Fuel consumption convergence for Case Study 1. ....	55
Figure 18: Nodal pressures simulated for Case Study 1. ....	56
Figure 19: Case Study 2, analogous to Leong and Ayala (2013). ....	58
Figure 20: Linear-Analog characteristic matrix for Case Study 2.....	60
Figure 21: Pressure convergence for Case Study 2. ....	61
Figure 22: Efficiency convergence for Case Study 2. ....	62
Figure 23: Compressor rotation velocity convergence for Case Study 2. ....	63
Figure 24: Flow moving through compression station for Case Study 2. ....	64
Figure 25: Fuel consumption convergence for Case Study 2. ....	64
Figure 26: Horsepower usage convergence for Case Study 2. ....	65
Figure 27: Nodal pressures simulated for Case Study 2. ....	65
Figure 28: Case Study 3.....	66
Figure 29: Case Study 3.a .....	69
Figure 30: Case Study 3.a .....	70
Figure 31: Case Study 3.b.....	71
Figure 32: Case Study 3.c. ....	72
Figure 33: Case Study 3.d.....	73
Figure 34: Case Study 3.e. ....	74
Figure 35: Case Study 3.f: .....	75
Figure 36: Case Study 3.f: . ....	76

Figure 37: Large natural gas transportation system. .... 79

.

**LIST OF TABLES**

Table 1: Friction factor formulas for different types of equations.....	18
Table 2: Height of different nodes of the system.....	53
Table 3: Dimensions of network pipes. ....	53
Table 4: Height of different nodes in the system.....	59
Table 5: Dimensions of network pipes. ....	59
Table 6: Dimensions of network pipes. ....	68
Table 7: Characteristics of the compression stations.....	68
Table 8: Optimal pressure distribution for case study 3. ....	76

## LIST OF SYMBOLS

$q_{Gscij}$ : flow between nodes  $i$  and  $j$  [SCFD]

$C_{ij}$ : pipe Conductivity [SCFD/psia]

$L_{ij}$ : pipe Linear Analog Conductivity [SCFD/psia]

$\sigma$ : unit dependent constant for the generalized gas flow equation

$SG_g, \gamma$ : gas specific gravity [-]

$T_{av}$ : average absolute temperature [DEG R]

$z_{av}$ : average compressibility factor [-]

$T_{sc}$ : temperature at standard conditions [DEG R]

$P_{sc}$ : pressure at standard conditions [psia]

$f$ : fanning friction factor [-]

$L_e$ : pipe equivalent length [miles]

$d$ : pipe internal diameter [in]

$P_i$ : pressure at node  $i$  [psia]

$k_w, k_{PA}, k_{PB}$ : unit – dependent constant for gas friction factor equations [-]

$R_e$ : Reynolds number [-]

$\rho$ : gas density [lbm/ft<sup>3</sup>]

$\mu_g$ : fluid dynamic viscosity [cP]

$v$ : fluid velocity [ft/s]

$P_{av}$ : pipe branch average pressure [psia]

$C_{cij}$ : compressor constant  $\left[ \frac{SCFD}{HP} \right]$

$r_{cij}$ : compression ratio [-]

$n_p$ : polytropic coefficient [-]

$n_a$ : adiabatic coefficient [-]

$n$ : compressor coefficient [-]

$k$ : number of compression stations [-]

$n_{st}$ : number of compression stages [-]

$\eta$ : compressor efficiency [-]

$HP$ : horsepower [HP]

$T_{suction}, T_i$ : temperature at entry of compressor [DEG R]

$T_{discharge}$ : temperature at discharge of compressor [DEG R]

$z_{suction}$ : compressibility of fluid entering compressor [-]

$z_{discharge}$ : compressibility of fluid leaving compressor [-]

$z_{av}$ : fluid average compressibility factor [-]

$P_{suction}$ : pressure at entry of compressor [psia]

$P_{discharge}$ : pressure at discharge of compressor [psia]

$H$ : compressor head [lbf - ft/lbm]

$Q$ : compressor inlet flow [ft<sup>3</sup>]

$\Delta H$ : elevation [ft]

$S$ : rotation velocity [rpm]

$S$ : supply at a certain node [SCFD]

$D$ : demand at a certain node [SCFD]

$g$ : gravitational Acceleration [ft/s<sup>2</sup>]

$g_c$ : unit conversion factor [lbm - ft/lbf - s<sup>2</sup>]

$\omega$ : initial guess of  $L_{ij}$  with respect to  $C_{ij}$

## ACKNOWLEDGEMENTS

To my advisor, Dr. Luis Ayala, who I have learned to see not only as an academic supervisor, but as a dear friend whose counseling goes beyond the laws of physics. Thanks for being a source of guidance in the hours of most need.

To Dr. Ertekin and Dr. Emami, for the honor of having them in my thesis committee and for the great insights provided to this study.

To my parents, Maria Rita and Antônio Carlos, for all their support and love that have pushed me forward in all aspects of life.

To my siblings Thales, Sheila, Fabiana and Samir, for all actions and words of encouragement.

To my uncles and aunts, who have taught me that family values are concepts way more profound than mere social norms. In special, thanks to Gláucia, Gustavo, Itamar, Dalva, Cirene and Marly.

To my great friends at the Pennsylvania State University, Renzo and Giancarlo. Thanks for the help and companionship, always present and available.

To Dr. Molina, who first introduced me to the world of science: always a master and advisor.

To my friends whose presence are of great support, no matter the distance: Maristela, Maíra, Vinícius Mourão and Elaine.

Especially, thanks to Dona Zita (in memorian). Dear grandmother, poet, story teller, counselor and inspirer of minds and souls.

Finally, to all people who made my experience at Penn State unforgettable:

I will be eternally thankful!

## CHAPTER 1

### INTRODUCTION

Gas transportation is one of the most studied topics of natural gas engineering. It concerns the network of elements that move gas from wells to the final consumers as it flows through the different components of the system such as pipelines, valves, pipe legs, and compressors. The points where these different components connect are called nodes. The connection elements are called branches. Most of the work developed in natural gas transportation focuses on simulation of how pressures are to be found in each node of the system, given its supplies, demands, and physical characteristics (Menon, 2005).

In general, transportation systems can be very large and account for a variety of components that extend through miles of pipelines. As an example, Figure 1 displays how the natural gas transportation system was distributed in the US during 2008.

Since gas networks are usually very large and pressure is reduced during fluid flow due to energy losses, compression stations are necessary at some points of the system in order to compress the gas and regain pressure.

Compression stations, in which one or more compressors might be present, have their performance constrained by compressor efficiency. While some authors have used the approximation of efficiency to constant values (Leong and Ayala, 2012), others have proposed the use of polynomial approximations of efficiency curves in order to estimate efficiency for a given compressor (S. Wu, 1998; Wu et al., 2000). These efficiency curves,

also referred to as compressor performance curves, have the characteristic of being highly non-linear.

Furthermore, when compressors are present in a network, they usually consume part of the gas flowing through the network in order to produce enough power for the compressor itself to work. This can result in great expenses with gas consumption (Rios-Mercato and Borraz-Sanchez, 2015).

S. Wu (1998) estimated that about 3-4% of the gas transported in a network is consumed in the compression stations. S. Wu (1998) also indicated that 25% to 50% of the operational cost of the companies that manage natural gas transportation networks is related to gas consumption in compression stations. This cost is related to all recurrent administration expenses that are verified on a day-to-day basis, such as costs on employees, water, and, in this case, gas consumption. This implies that the effective minimization of fuel consumption could result in savings of great magnitude for the midstream industry.

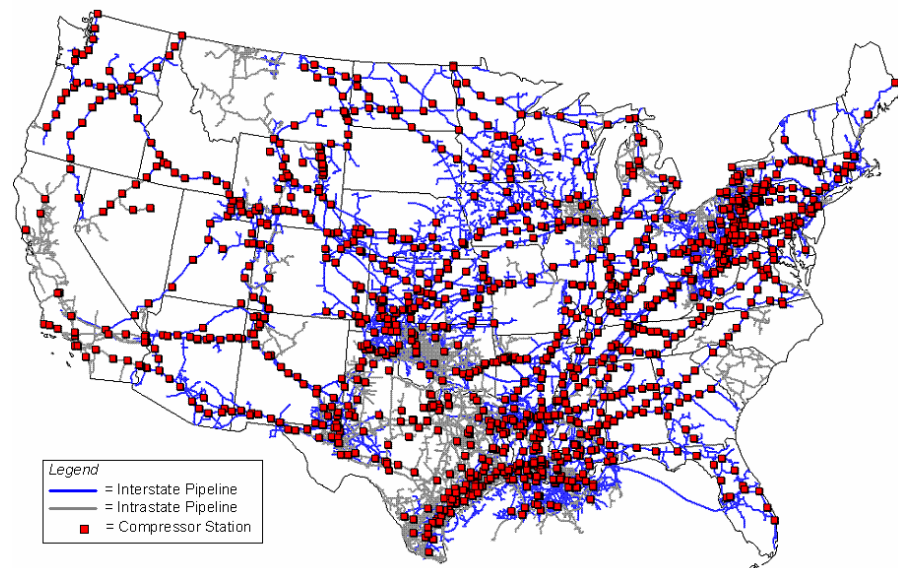


Figure 1: U.S. natural gas pipeline networks. Source: Energy Information Administration (2016).

However, the minimization of natural gas transportation presents the challenge of an optimization formulation that relies largely on a highly non-linear system of equations. Moreover, most of the methods found in literature that target the solution of such equations are dependent on reliable initial guesses of nodal pressures or flowrates moving through the branches of the network. This is the case of the Newton-Raphson method, which could lead to an undesired, non-converging scenario.

In order to provide a proper solution for the challenges aforementioned, this study focuses on:

- Simulating the pressures of different nodes of a system;
- The estimation of fuel consumption for a given transportation system;
- The estimation of compressor efficiency by the use of polynomial compressor performance curves and;
- The minimization of fuel consumption in a natural gas transportation system.

All procedures are implemented by the use of a linearization method named the Linear Analog, developed by Leong and Ayala (2012), which simplifies the simulation of pressure distribution in a given network by not requiring initial guesses of nodal pressures for its iterative process.

In order to present methods and results in a practical manner, this paper is structured as follows:

In Chapter 2, a literature review on natural gas networks is presented, covering topics such as gas flow equations, gas network nodal analysis, friction factors, Reynolds

number, and temperature changes during gas compression. The Linear Analog method developed by Leong and Ayala (2012) is also introduced and discussed.

In Chapter 3, the topic of gas compression is discussed, and the compressor equation is presented. The equations for compressor performance according to Wu et al. (2000) are also introduced.

In Chapter 4, the optimization problem for planning of natural gas transportation is discussed as presented by S. Wu (1998), with especial attention for the gas consumption function and the compressor equation domain.

In Chapter 5, the methodology used to solve the calculations of fuel consumption and to develop the optimization problem is explained, with description of the domain-constrained search procedure.

In Chapter 6, the methods introduced are applied to three different case studies along with the presentation of results and discussion.

In Chapter 7, some concluding remarks are provided and future work is proposed.

## CHAPTER 2

### LITERATURE REVIEW

One of the most basic problems in natural gas transportation concerns the calculation of pressures at upstream and downstream nodes of a single pipe, as well as the flow going through it (Ayala, 2013; Kumar, 1987; Larock et al., 2000; Leong and Ayala, 2013; Osiadacz, 1987). This problem corresponds to the development of a mathematical model that will describe fluid flow in pipelines (Ayala, 2013; Kumar, 1987; Larock et al., 2000; Leong and Ayala, 2013; Osiadacz, 1987) and captures how physical properties of the pipe and of the flowing fluid will affect the capability that the pipe has to transport gas and how conductible this pipe will be according to these properties.

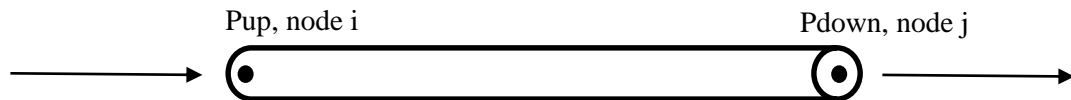


Figure 2: Scheme of flow going through the two nodes of a pipeline.

In Figure 2, a basic scheme of fluid transportation is presented. In this scheme, gas flows through a horizontal pipe according to pipe and fluid characteristics and pressure conditions at the pipe inlet, conventionally called node i, or upstream node; and pressure conditions at the pipe outlet, conventionally called node j, or downstream node.

A variation of the case shown in Figure 2 is the non-horizontal, inclined pipe. While in the horizontal case, pressure is mainly affected by energy losses due to the friction of the fluid against the pipe wall, in the inclined case, depicted in Figure 3, pressure is also affected by gravitational forces related to the differences of height ( $\Delta H = \text{elevation}$ ) between node i, upstream; and node j, downstream (Ayala, 2013; Ikoku, 1984).

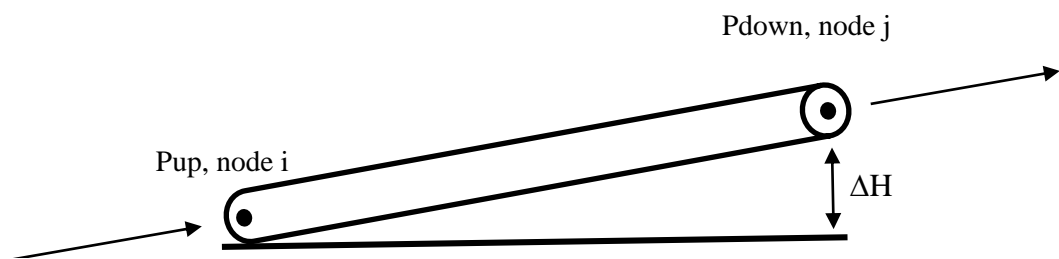


Figure 3: Scheme of flow going through the two nodes of an inclined pipeline.

If the schemes in Figures 2 and 3 represent pipes with the same physical properties, flowing fluid characteristics, and initial pressure at node i, it can be concluded that node j in Figure 3 will have a pressure value that is smaller than the one found in node j of Figure 2. In Figure 3, pressure will be lost along the flowline not only due to energy losses related to friction, but also due to energy losses related to gravitational forces.

In order to develop an equation that is capable of describing the gas flow through both horizontal and inclined pipes, different attempts have been presented (Ayala, 2013; Ikoku, 1984). As a result, different equations have been proposed with slight differences between each, mostly related to the calculation of the parameter that determines friction

losses, also known as friction factor. These equations can be summarized in a generalized form that is derived from the First and Second Laws of Thermodynamics (Ayala, 2013).

## 2.1 The Gas Generalized Pipe Flow Equation Derivation

The generalized equation for gas flow in pipes can assume two basic different forms: the Q-explicit form; or the  $\Delta P$ -explicit form. This study is based on the Q-explicit form of the generalized equation for gas flow. However,  $\Delta P$ -explicit form will be briefly discussed in this chapter.

From the combination of the First and Second Laws of Thermodynamics, it can be stated that the pressure loss of fluid flow in pipes can be described by equation 1 (Brill and Mukherjee, 1999):

$$\left(\frac{dp}{dx}\right)_T = \left(\frac{dp}{dx}\right)_e + \left(\frac{dp}{dx}\right)_a + \left(\frac{dp}{dx}\right)_{lw}$$

*equation 1*

where:

$\left(\frac{dp}{dx}\right)_T$  accounts for the total pressure loss taking place during fluid flow.

$\left(\frac{dp}{dx}\right)_e$  accounts for pressure losses due to changes in elevation.

$\left(\frac{dp}{dx}\right)_a$  accounts for pressure losses due to changes in acceleration.

$\left(\frac{dp}{dx}\right)_{lw}$  accounts for pressure losses due to friction of the fluid against the pipe wall.

Ayala (2013) demonstrates that equation 1 can be rewritten in terms of other variables and manipulated in order to give:

$$\frac{dp}{\rho} = -\frac{v}{g_c} dv - \frac{g}{g_c} dz - dlw$$

*equation 2*

where:

$p$  represents pressure;

$\rho$  represents the fluid density;

$v$  represents fluid velocity;

$g$  represents gravity acceleration;

$g_c$  represents a conversion factor;

$lw$  represents lost work to the environment, also known as irreversible loss.

By manipulating density, and differentiating it with respect to space  $dx$ , equation 2 will collapse to:

$$\frac{dp}{dx} = -\frac{\rho v}{g_c} \frac{dv}{dx} - \frac{\rho g}{g_c} \frac{dz}{dx} - \rho \frac{dlw}{dx}$$

*equation 3*

Then, equation 3 can be related to equation 1 by the observation that:

$$\left(\frac{dp}{dx}\right)_e = -\frac{\rho g}{g_c} \frac{dz}{dx}$$

*equation 4*

$$\left(\frac{dp}{dx}\right)_a = -\frac{\rho v}{g_c} \frac{dv}{dx}$$

*equation 5*

$$\left(\frac{dp}{dx}\right)_{lw} = -\rho \frac{dlw}{dx}$$

*equation 6*

This is consistent with the derivations found in the work of Ayala (2013). Ayala (2013) also indicated that, for pipes,  $dlw$  is equivalent to the pressure loss due to the shear stress between the pipe wall and the fluid, elucidating that:

$$\left(\frac{dp}{dx}\right)_{lw} = -\rho \frac{dlw}{dx} = -\tau_w \frac{\pi d}{A}$$

*equation 7*

where:

$\tau_w$  is the shear stress of the fluid against the pipe wall;

$d$  is the pipe diameter;

$A$  is the pipe cross-sectional area.

where:

$$A = \frac{\pi d^2}{4}$$

*equation 8*

Also, according to Ayala (2013), shear stress can be calculated by the following equation:

$$\tau_w = \frac{f_F \rho v^2}{2g_c}$$

*equation 9*

where  $f_F$  is the Fanning friction factor.

If equations 9 and 8 are combined into equation 7, equation 10 is true with regards to losses due to friction:

$$\left(\frac{dp}{dx}\right)_{lw} = \left(\frac{dp}{dx}\right)_f = -\frac{2f_F \rho v^2}{g_c d}$$

*equation 10*

However, it is noteworthy that velocity can be written in terms of mass flow, as follows:

$$vA = \frac{m}{\rho}$$

*equation 11*

where  $m$  is the mass flow.

Equation 11 can be modified to give:

$$v = \frac{m}{\rho A}$$

*equation 12*

Finally, equation 12 can be plugged into equation 10 and manipulated in order to result in:

$$\left(\frac{dp}{dx}\right)_{lw} = \left(\frac{dp}{dx}\right)_f = -\frac{2f_F m^2}{g_c d A^2 \rho}$$

*equation 13*

Taking equation 3 in consideration again, the contribution of acceleration forces to pressure (energy) losses in pipe fluid flow is so small that it can be neglected. This will lead to the following:

$$\left(\frac{dp}{dx}\right)_T = \left(\frac{dp}{dx}\right)_e + \left(\frac{dp}{dx}\right)_{lw} = \left(\frac{dp}{dx}\right)_e + \left(\frac{dp}{dx}\right)_f$$

*equation 14*

By substituting equations 4 and 13 into equation 14, it can be found that:

$$\left(\frac{dp}{dx}\right)_T = -\frac{\rho g dz}{g_c dx} - \frac{2f_F m^2}{g_c d A^2 \rho}$$

*equation 15*

For inclined pipes, it is relevant to highlight that the variation in inclination is a function of height differences between height at downstream node and upstream node, as demonstrated in Figure 4:

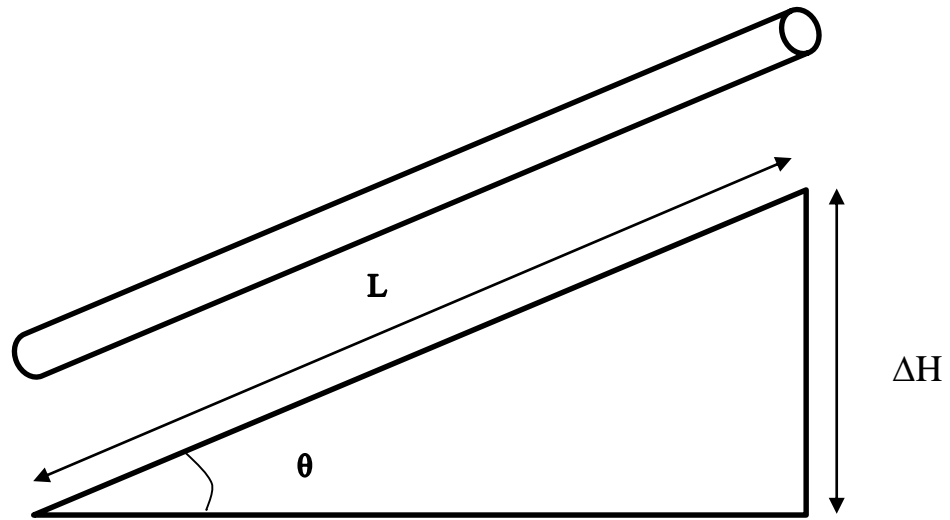


Figure 4: Trigonometric behavior of inclined pipes

where  $L$  is the pipe length.

Furthermore, it can be stated that:

$$\sin \theta = \frac{dz}{dx} = \frac{\Delta H}{L}$$

*equation 16*

where  $dz$  represents variation in height.

Adding equation 16 into equation 15, it can be observed that:

$$\left(\frac{dp}{dx}\right)_T = -\frac{\rho g \Delta H}{g_c L} - \frac{2f_F m^2}{g_c d A^2 \rho}$$

equation 17

With a little bit of manipulation and the observation that:

$$A^2 = \frac{\pi^2 d^4}{16}$$

equation 18

equation 17 can be rewritten as:

$$\rho dp = -\frac{32f_F m^2}{g_c d^5 \pi^2} dx - \frac{\rho^2 g \Delta H}{g_c L} dx$$

equation 19

All terms but density are constant in equation 19. This means that if equation 19 is integrated on both sides, it will give:

$$\int_{\rho_1}^{\rho_2} \rho dp = -\frac{32f_F m^2}{g_c d^5 \pi^2} \int_0^L dx - \frac{g \Delta H}{g_c L} \int_0^L \rho^2 dx$$

equation 20

Ayala (2013) suggests the following manipulation for integration of equation 20:

$$\alpha = \frac{32f_F m^2}{g_c d^5 \pi^2}$$

equation 21

and:

$$\beta = \frac{g\Delta H}{g_c L}$$

*equation 22*

If equations 21 and 22 are coupled into equation 19, then:

$$\rho dp = -\alpha dx - \beta \rho^2 dx$$

*equation 23*

and consequently:

$$dp = -\frac{\alpha dx}{\rho} - \beta \rho dx$$

*equation 24*

Equation 24, by preserving pressure-density dependence upon integration, is consistent with the work of Ferguson (1936). It can also be manipulated in order to provide:

$$-dx = \frac{dp}{\left(\frac{\alpha}{\rho} + \beta \rho\right)}$$

*equation 25*

From real gas law, it can be observed that:

$$\phi = \frac{MW_{gas}}{z_{av}RT_{av}}$$

*equation 26*

where:

$MW_{gas}$  is the molecular weight of the gas (lbm/lbmol)

$R$  is the universal gas constant (psi-ft / lbmol-°R)

$T_{av}$  is the temperature (°R)

$z_{av}$  is the average compressibility factor of gas.

Coupling equations 25 and 26, it can be arrived at:

$$-\int_0^L dx = \int_{P_1}^{P_2} \frac{P dp}{\left(\frac{\alpha}{\phi} + \phi\beta P^2\right)}$$

*equation 27*

Upon integration, equation 27 will result in the generalized gas flow equation:

$$q_{Gscij} = C_{ij}(P_i^2 - e^s P_j^2)^n$$

*equation 28*

where:

$$C_{ij} = \frac{\sigma}{\sqrt{SG_g T_{av} Z_{av}}} \left( \frac{T_{sc}}{P_{sc}} \right) \left( \sqrt{\frac{1}{f}} \right) \frac{d^{2.5}}{Le^{0.5}}$$

*equation 29*

$$\sigma = \sqrt{\frac{\pi^2 R g_c}{64 MW_{air}}}$$

*equation 30*

$$s = \frac{2 g \Delta H \gamma_{gas} MW_{air}}{g_c z_{av} R T_{av}}$$

*equation 31*

$$L_e = \frac{(e^s - 1)}{s} L$$

*equation 32*

Equation 28 is the generalized gas flow equation in Q-explicit form, which accounts for energy losses due to both friction and elevation changes. This equation can also be written in terms of  $\Delta P$ -explicit.

## 2.2 The Generalized Gas Flow Equation in $\Delta P$ -explicit form

$\Delta P$ -explicit formulation will not be used in the developments herein presented. However, it is noteworthy that equation 28 can be manipulated in order to give the generalized gas flow equation in  $\Delta P$ -explicit form:

$$P_i^2 - P_j^2 = R_g q_{Gscij} \frac{1}{n}$$

*equation 33*

where:

$$R_g = r_G \frac{L_e}{d^m}$$

*equation 34*

And:

$$r_G = \frac{\gamma_{gas} T_{av} Z_{av}}{\sigma^2} f_F \left( \frac{P_{sc}}{T_{sc}} \right)^2$$

*equation 35*

Where  $m$  and  $n$  will vary according to the friction factors being used.

### 2.3 Friction Factors

Different forms of calculating the friction factor ( $f$ ) have been proposed. For the effects of this work, Weymouth, Panhandle-A, Panhandle-B, AGA Fully-Turbulent, and Colebrook's Equation with rigorous friction factor calculations will be presented. Each of these formulas are displayed in Table 1.

Gas-flow Equation	Friction-Factor Expression
Colebrook (1939)	$\frac{1}{\sqrt{f}} = -4 \log_{10} \left( \frac{e/d}{3.7} + \frac{5.02}{Re\sqrt{f}} \right)$
Weymouth (1912)	$f_F = \frac{k_w}{d^{1/3}}$
Panhandle-A (original Panhandle) (Boyd, 1983; GPSA, 2004)	$f_F = \frac{k_{PA}}{\left( \frac{q_{Gsc} S G_g}{d} \right)^{0.1461}}$
Panhandle-B (modified Panhandle) (Boyd, 1983; GPSA, 2004)	$f_F = \frac{k_{PB}}{\left( \frac{q_{Gsc} S G_g}{d} \right)^{0.03922}}$
AGA (fully turbulent) (AGA, 1965)	$\frac{1}{\sqrt{f}} = 4 \log_{10} \left( \frac{3.7d}{e} \right)$

Table 1: Friction factor formulas for different types of equations.

It is also important to notice that the generalized gas flow equation can admit different units according to the  $\sigma$  parameter used. For the effects of this work, field units will be used as stated in the nomenclature (list of symbols) section, and the following values are to be implemented in the formulas presented in this section:

$$k_w = 0.002352 [in^{1/3}]$$

$$k_{PA} = 0.01923 \left[ \left( \frac{SCFD}{in} \right)^{0.1461} \right]$$

$$k_{PB} = 0.00359 \left[ \left( \frac{SCFD}{in} \right)^{0.03922} \right]$$

$$\sigma = 2,818 \left[ \sqrt{\frac{\text{psi-ft}^3 (\text{lbm-ft/lbf-s}^2)}{\text{lbmol-}^\circ\text{R} \left(\frac{\text{lbm}}{\text{lbmol}}\right)}} \right]$$

### 2.3.1 Colebrook Formula

In Colebrook's (1939) equation, Reynolds number needs to be calculated. The formula of Reynolds number is given by:

$$R_e = \frac{\rho v d}{\mu_g}$$

*equation 36*

where  $\mu_g$  , gas viscosity, can be calculated by the formula provided by Lee, Gonzalez and Eakin (1966).

$$\mu_g = 1 * 10^{-4} k_v \text{EXP} \left( x_v \left( \frac{\rho_g}{62.4} \right)^{y_v} \right)$$

*equation 37*

where:

$$k_v = \frac{(9.4 + 0.02 MW_g) T^{1.5}}{209 + 19 MW_g + T}$$

*equation 38*

$$x_v = 3.5 + \frac{986}{T} + 0.01MW_g$$

*equation 39*

For the calculation of density, real gas law will be used and the system's average pressure will be needed. The pressure to be used is branch average pressure, also known as  $P_{av}$  (Ayala, 2013), calculated by equation 40:

$$P_{av} = \frac{2}{3} \left( P_1 + P_2 - \frac{P_1 P_2}{P_1 + P_2} \right)$$

*equation 40*

## 2.4 Gas Network Analysis

As mentioned previously, gas network analysis concerns the series of procedures for which the flows in a network of pipes can be calculated. It also concerns the estimation of pressures in each one of the nodes in the network (Ayala, 2013; Kumar, 1987; Larock et al., 2000; Leong and Ayala, 2013; Osiadacz, 1987).

In gas network analysis, material balance equations are computed at each node in order to obtain a system of equations that can be solved for pressures or flowrates. For the cases of systems with compressors, the equation that describes the flow through the compressors is added to the material balance equations.

In general, a nodal network is composed of three basic elements:

- Nodes, commonly referred to as N;
- Branches or pipes, which in this work are referred to as B and;
- Loops, commonly referred to as L.

The number of nodes (N), the number of branches (B), and the number of loops (L) can be related by equation 41:

$$B = (N - 1) + L$$

*equation 41*

For example, the pipe segment shown in Figure 1 has two nodes and zero loops. Thus, it has one branch. Two main approaches exist in order to develop the system of flow equations for a nodal network. The nodal-loop formulation, also known as the Q-formulation, and the nodal formulation, also known as the P-formulation. They are based, respectively, on the general equations demonstrated in sections 2.4.1 and 2.4.2 of this chapter.

#### 2.4.1 The Nodal-loop Formulation or Q-formulation

The nodal-loop formulation is focused on calculating the flowrate going through each pipe before knowing the pressure values at each node. It consists on a series of material balance equations at each node and energy conservation equations at each loop of a network.  $(N - 1)$  equations linearly independent can be obtained from nodal mass conservation:

$$\sum_{i=1}^N q_{in,i} - \sum_{i=1}^N q_{out,i} + S - D = 0$$

equation 42

L loop equations are obtained from energy conservation at each loop of a network:

$$\sum_{i=1}^N (P_i^2 - P_j^2) = \sum_{ij} \left( R_g q_{Gscij} \frac{1}{n} \right) = 0$$

equation 43

As it can be observed from equation 41, the final system will be comprised of B equations. Once solved, this system will be able to determine flowrates going through each one of the pipe segments.

#### 2.4.2 The Nodal Formulation or P-formulation

While the Q-formulation concerns the solution of a system that will have as output answers the flowrates going through each segment of a pipe, the P-formulation will impose nodal material balance equations in terms of pressures, and then solve the system for pressures.

Basically, it will solve the following system:

$$\sum_{i=1}^N q_{in,i} - \sum_{i=1}^N q_{out,i} + S - D = \sum_{i=1}^N C_{ij} (P_i^2 - e^s P_j^2)^n - \sum_{i=1}^N C_{ij} (P_i^2 - e^s P_j^2)^n + S - D$$

equation 44

This system will have (N - 1) linearly independent nodal equations, but N (pressure) unknowns. In order to provide linear balance for the system, one more equation is necessary, or one unknown needs to be removed. In this case, one of the pressures is usually specified.

## 2.5 Solution Procedures

A series of solution procedures have been proposed for solving these systems of nodal equations. The most common are the Linear Theory Method (Wood and Carl, 1972), the Newton-Raphson Method (Press et al., 2007), the Hardy Cross Method (Cross, 1932) and the Linear-Pressure Analog Method (Leong and Ayala, 2012), commonly referred to as the Linear Analog method. Of these methods, Newton-Raphson is largely used since it possesses fast convergence and can also be numerically determined. However, Newton-Raphson implies the need for a “good initial guess”, close to the actual value of the variables being analyzed. Poor initial guesses might actually lead to a non-convergence scenario.

### 2.5.1 The Newton-Raphson Method

The Newton-Raphson Method for multivariable equations is given as follows:

For a certain vector of n equations  $f$ .

$$f = [f_1, f_2, f_3, f_4, \dots, f_n]$$

*equation 45*

a vector of n variables:

$$\bar{x} = [ x_1, x_2, x_3, x_4, \dots, x_n ]$$

*equation 46*

and a Jacobian vector:

$$J_F = \nabla_f(\bar{x}) = J_{ij} = \frac{\partial f_i}{\partial x_j}$$

*equation 47*

the system solution is given by the operation:

$$\bar{x}_{new} = \bar{x}_{old} - J_F^{-1}(\bar{x}_{old})f(\bar{x}_{old})$$

*equation 48*

### 2.5.2 The Linear Analog Method

The Linear Analog method is an elegant algorithm developed to solve systems of nodal equations derived from the material balance of natural gas transportation systems. The Linear Analog advantage relies on the fact that it does not require an initial guess of pressures or flowrates in order to assure convergence. This is the method for the solution of the system of equations for gas flow that is implemented in this study.

The algorithm procedure of the Linear Analog method was presented by Leong and Ayala (2012). Its basis relies on the linearization of the gas flow equation in Q-explicit

form, where the gas flow is treated as analogous to laminar flow, allowing for the flow equation to become much simplified, as shown in equation 49.

$$q_{Gscij} = C_{ij}(P_i^2 - e^s P_j^2)^n = L_{ij}(P_i - P_j)$$

*equation 49*

where  $L_{ij}$  is the Linear Analog pipe conductivity and:

$$L_{ij} = T_{ij} * C_{ij}$$

*equation 50*

$$T_{ij} = \sqrt{1 + \frac{2}{r_{ij} - 1}}$$

*equation 51*

$$r_{ij} = \frac{P_i}{e^{\frac{s}{2}} P_j}$$

*equation 52*

The derivation of  $T_{ij}$  is given in Figure 5, extracted from the work of Leong and Ayala (2012).

This method relies on the fact that  $L_{ij}$  can assume an initial value equal or greater than  $C_{ij}$  and approaches its correct value each time that the system of equations is solved during the Linear Analog iterations. At each new iteration, the value of  $T_{ij}$  is updated and

consequently the value of  $L_{ij}$  is also updated, until convergence is achieved. Figure 6 shows the algorithm of the Linear Analog as it was presented by Leong and Ayala (2012).

$$\begin{array}{c}
 q_{Gij} = L_{ij}(p_i - p_j) \qquad q_{Gij} = C_{ij}(p_i^2 - p_j^2)^{0.5} \\
 \swarrow \qquad \searrow \\
 L_{ij}(p_i - p_j) = C_{ij}(p_i^2 - p_j^2)^{0.5} \\
 \downarrow \\
 \frac{L_{ij}}{C_{ij}} = \frac{(p_i - p_j)(p_i + p_j)}{(p_i - p_j)(p_i^2 - p_j^2)^{0.5}} \\
 \downarrow \\
 \frac{L_{ij}}{C_{ij}} = \left( \frac{\frac{p_i}{p_j} + 1}{\frac{p_i}{p_j} - 1} \right)^{0.5} \qquad \text{Let } r_{ij} = \frac{p_i}{p_j} \\
 \frac{L_{ij}}{C_{ij}} = \left( \frac{r_{ij} + 1}{r_{ij} - 1} \right)^{0.5} \\
 \frac{L_{ij}}{C_{ij}} = \sqrt{1 + \frac{2}{r_{ij} - 1}} \qquad \text{Let } T_{ij} = \sqrt{1 + \frac{2}{r_{ij} - 1}} \\
 L_{ij} = T_{ij}C_{ij}
 \end{array}$$

Figure 5: Derivation of the Linear-Analog conductivity. Source: Leong and Ayala (2012).

Besides not requiring initial guesses for nodal pressures or flowrates, the Linear Analog also is a linearly converging method. This implies that the method does not face the problems of non-convergence such as does Newton-Raphson. Therefore, once applied to gas networks analysis, this method, though requiring more iterations to converge than

does Newton-Raphson, has an application that does not rely on initial guesses, or “good” initial guesses (for nodal pressures) in order to guarantee convergence.

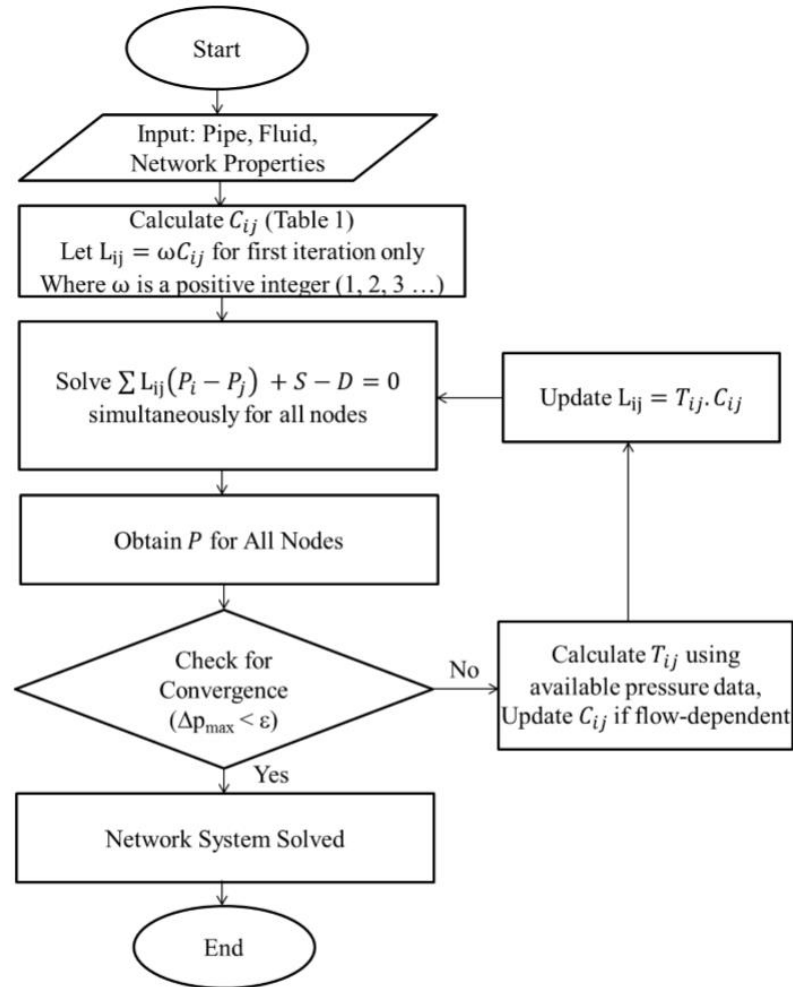


Figure 6: The Linear-Pressure Analog algorithm. Source: Leong and Ayala (2012).

The Linear Analog method is especially useful for large networks with many components such as wells and compression stations, for which equations are very non-linear and good initial guesses are needed for a variety of pressure nodes, possibly leading the computer code used to automate the procedure to a non-convergence state.

The Linear Analog method, thus, is a powerful tool for testing different scenarios of network performance. It makes it possible, for example, to test a system with one compressor for different values of compression ratios, without the concern of providing the code with initial guesses for nodal pressures.

## **CHAPTER 3**

### **THE COMPRESSOR**

The compressor is one of the most important pieces of equipment in a network of natural gas transportation, especially in networks where pipes are very long. This importance relies on the principle of pressure loss (energy loss) discussed in Chapter 2. As gas travels through a pipeline, it starts to lose pressure along the way, mainly due to the friction of the fluid against the pipe wall. Nevertheless, it is important that, in a network, pressure is not allowed to go beyond a certain lower limit. If pressure becomes too low, the energy, and therefore the expense necessary to increase pressure in later sections of the network, becomes excessively high. One way to remedy this situation is through the use of compressors.

A compressor is a device that is used to increase the pressure of a compressible fluid (Brown, 2005). There are different types of compressors, but mainly two types are more commonly used in the natural gas transportation industry: centrifugal compressors and reciprocating compressors. The type being analyzed in this study is the centrifugal compressor, which rotates the gas entering through it in order to increase its velocity and thus its pressure. It is one of the most used types of compressors for compression of oil-free gas (Block, 1933).

A centrifugal compressor is also called a radial-flow compressor, and it is widely used and typically found in a multi-stage system in which compressors are placed in series (Brown, 2005). The gas enters the compressor through a suction node, located right at the

compressor entrance, and leaves the compressor through a discharge node, found right at the exit of the compressor. According to Brown (2005), during this process, an impeller consisting of radial or backward-leaning blades rotates, moving gas from between the rotating blades radially and outward to discharge. Energy is transferred to the gas while it is traveling through the impeller, converting part of the energy to pressure.

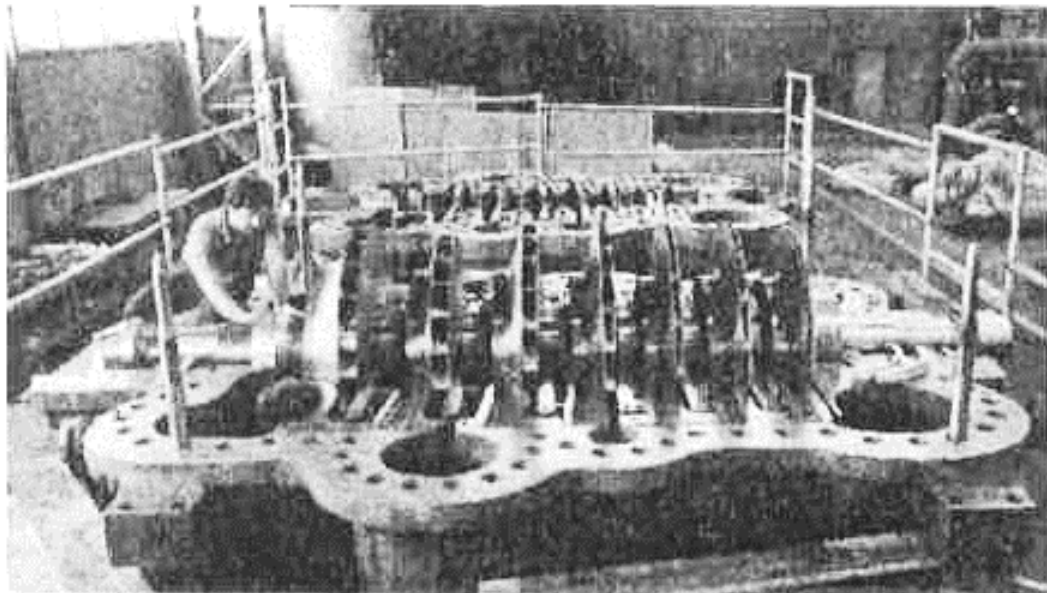


Figure 7: Radial-flow horizontally split multistage centrifugal compressor. Source: Brown (2005).

Gresh (2001) discusses that centrifugal compressors have advantages and disadvantages. The advantages are the possibility of a wide operating range, low maintenance needs, and high reliability. Disadvantages include instability at low flow and moderate efficiency values.

A scheme of a compressor in a network is depicted in Figure 8.

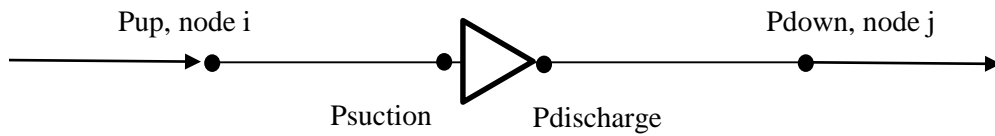


Figure 8: Scheme of a compressor coupled to a Natural Gas Transportation Network

Where the compression ratio is given by Equation 53

$$r_{cij} = \frac{P_{discharge}}{P_{suction}}$$

*equation 53*

In Figure 9, the image of a centrifugal compressor is presented:



Figure 9: Centrifugal gas compressor. Source: Caterpillar Company (2016)

It is important to note, however, that it is very unlikely that a certain branch of a network would be designed to flow gas through only one compressor, but rather this

process is performed in stages, through a series of compressors. This operation is necessary because, usually, increasing the pressure of gas will increase the collision of molecules, adding energy to the system. Part of the energy added is then transformed into heat, with an observed rise in temperature, making the temperature increase as pressure is increased.

With compression performed in stages, gas can go through intercoolers between different compressors at a station in order to mitigate the changes in temperature. This will prevent temperature from reaching a certain maximum and mitigate risks, avoiding accidents that could take place if the temperature in the compressor becomes too high, such as the degradation of the lubrication fluid.

Figure 10 shows a compression station.



Figure 10: A compression station in Tapinhoa, Brazil. Source: Valerus Company (2016)

For the calculation of discharge temperatures at compressors, the formula provided by Menon (2005) is used. The formula is given by equation 54:

$$T_{discharge} = T_{suction} \left( \frac{z_{suction}}{z_{discharge}} \right) \left( \frac{P_{discharge}}{P_{suction}} \right)^{\frac{n-1}{n}}$$

equation 54

where n is the compressor coefficient.

### 3.1 Coupling of Compressor to the System

When compressors are present in a certain piping system, the strategy of Leong and Ayala (2012) is used: nodal material balance will take the compressor equation into consideration. The compressor equation is given by:

$$q_{Gij} = C_{cij}HP$$

equation 55

where:

$q_{Gij}$  is the volumetric flowrate going through the compressor.

$C_{cij}$  is the compressor constant.

$HP$  is the horsepower used by the compressor in order to perform work.

and:

$$C_{cij} = \frac{1}{k_c \left[ (r_{cij})^{\frac{n-1}{n}} - 1 \right]} * 10^6$$

equation 56

$$k_c = 0.0857 \left( \frac{n_{st}n}{n-1} \right) T_i (Z_{av}) \left( \frac{1}{\eta} \right)$$

equation 57

where:

$r_{cij}$  is the compression ratio.

$n_{st}$  is the number of compression stages in a compression station.

$n$  is the compressor coefficient, which can assume the values of the polytrophic coefficient ( $n_p$ ).

$T_i$  is the compressor inlet temperature.

$z_{av}$  is the average compressibility factor of the fluid.

$\eta$  is the compressor efficiency.

One of the variables of extreme importance in the compressor equation is the compression ratio  $r_{cij}$ , since this ratio will be determinant of the amount of horsepower required in order for the compressor to work.

### 3.2 The Compressor Efficiency

As mentioned in Chapter 1, compressor efficiency ( $\eta$ ) has been addressed in the literature by basically two different approaches: while some authors have used constant

efficiencies, others have performed efficiency calculations by the use of compressor performance curves.

Wu et al. (2000) provided the following polynomials for the calculation of both efficiency and rotation velocity in a centrifugal compressor:

$$\eta = A_E + B_E \left(\frac{Q}{S}\right) + C_E \left(\frac{Q}{S}\right)^2 + D_E \left(\frac{Q}{S}\right)^3$$

*equation 58*

where in order to calculate  $S$ , it is necessary to use the following polynomial:

$$\frac{H}{S^2} = A_H + B_H \left(\frac{Q}{S}\right) + C_H \left(\frac{Q}{S}\right)^2 + D_H \left(\frac{Q}{S}\right)^3$$

*equation 59*

where:

$H$  is the compressor head.

$S$  is the rotation velocity in compressor.

$Q$  is the actual volumetric flowrate entering the compressor.

Whenever volumetric flow at standard conditions needs to be changed to volumetric flow at actual conditions, real gas law will be used with the calculation of properties such as density and compressibility factor by the use of the methods provided by Dranchuk and Abou-Kassem (1975), which are widely known and used in the Oil & Gas Industry.

Wu et al. (2000) provided the following values for the empirical constants in equation 58.

$$A_E = 134.8055 [-]$$

$$B_E = -148.5468 \left[ \frac{rpm}{ft^3} \right]$$

$$C_E = 125.1013 \left[ \frac{rpm^2}{ft^6} \right]$$

$$D_E = -32.0965 \left[ \frac{rpm^3}{ft^9} \right]$$

Wu et al. (2000) also provided the following values for the empirical constants in equation 59.

$$A_H = 0.6824 * 10^{-3} \left[ \frac{(lbf - ft/lbm)}{rpm^2} \right]$$

$$B_H = -0.9002 * 10^{-3} \left[ \frac{(lbf - ft/lbm)}{\left( \frac{ft^3}{min} \right) rpm} \right]$$

$$C_H = 0.5689 * 10^{-3} \left[ \frac{(lbf - ft/lbm)}{\left( \frac{ft^3}{min} \right)^2} \right]$$

$$D_H = -0.1247 * 10^{-3} \left[ \frac{(lbf - ft/lbm) rpm}{\left( \frac{ft^3}{min} \right)^3} \right]$$

### 3.3 The Compressor Domain

A compressor is a mechanical piece of equipment. Thus, like all mechanical equipment, it is restricted by a series of mechanical constraints that allow for the equipment to work properly.

In a centrifugal compressor, the main restrictions are related to the rotation velocity and the volumetric flow moving through the equipment. As it can be rationalized, the rotation velocity has upper limit and lower limit restrictions. Also, there are upper and lower limits related to volumetric flow going through the compressor. The upper limits of rotation velocity and volumetric flow will define a constraint called “Stonewall”. The lower limits of rotation velocity and volumetric flow will define a condition called “Surge”.

$$S_{\min} \geq S \geq S_{\max}$$

*equation 60*

$$Q_{\min} \geq Q \geq Q_{\max}$$

*equation 61*

$$\text{Surge} \geq \frac{Q}{S} \geq \text{Stonewall}$$

*equation 62*

“Surge” and “Stonewall” restrictions are extremely important in order to guarantee proper calculations of compressor operating conditions.

Wu et al. (2000) analyzed “Surge” and “Stonewall” conditions for a centrifugal compressor and arrived at the analysis shown in Figure 11, which gives the domain of the compressor equation restricted by “Surge” and “Stonewall” conditions.

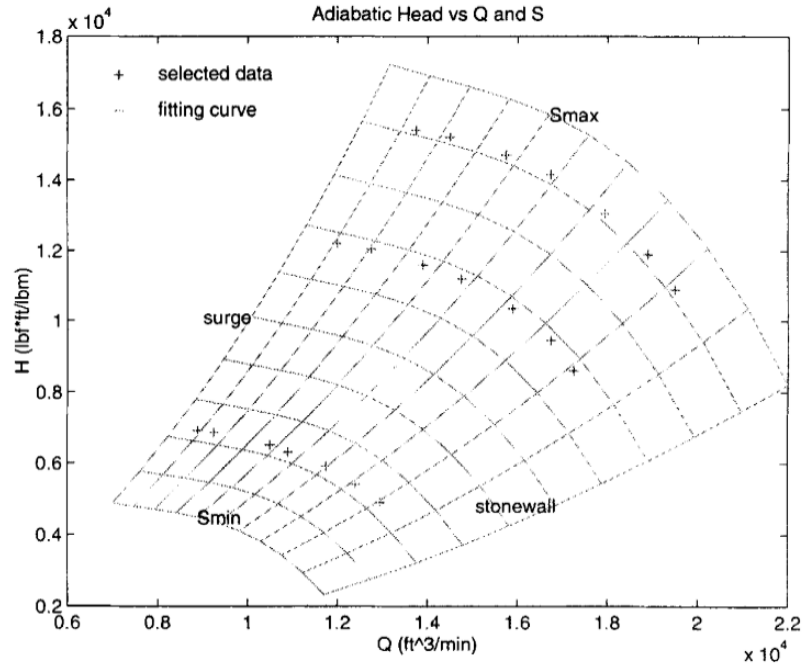


Figure 11: Compressor domain restricted to “surge” and “stonewall” conditions. Source: Wu et al. (2000)

## **CHAPTER 4**

### **THE COST MINIMIZATION MODEL**

One of the most comprehensive works on natural gas transportation was published by S. Wu (1998). The findings of the author were later aggregated to the discoveries of different authors and published by Wu et al. (2000). The works aforementioned presented a scientific problem of growing interest, which has been addressed in different ways by different authors. The problem is known as the fuel cost minimization problem.

#### 4.1 The Fuel Cost Minimization Problem

As discussed in the literature review, natural gas transportation networks are described mathematically by a system of equations that is, by nature, very non-linear. This non-linearity is intrinsically related to the fact that gas is a highly compressible fluid. The solution of this system of non-linear equations, as discussed in Chapter 2, relies on methods such as Newton-Raphson, which requires a good initial guess for nodal pressures or flowrates and thus does not provide guaranteed convergence. Yet, natural gas transportation in large networks demands compression stations that are expensive both in investment and in operation. The more compression required at compression stations, the more power needs to be used by the compressor and more gas needs to be burned in order to produce the work demanded. As mentioned in Chapter 1, Wu et al. (2000) estimated that about 2% to 5% of the gas transported in a large system is burned in the compression stations. Wu et al. (2000) also states that from 25% to 50% of the operational costs of

companies that manage gas transportation networks is spent on fuel for the compressor usage. Thus, a problem of great importance arises:

*How to set compressor operational parameters in a given network of gas transportation in such a way that the system will consume the minimum possible gas (fuel) in order to generate power for the compressors, under a given set of constraints.*

The difficulties of solving this problem rely on the following facts:

- The system of equations for a natural gas transportation network is highly non-linear;
- The objective function of this system, given by horsepower usage, is based on the compressor equation which is also very non-linear;
- Centrifugal compressors have “Surge” and “Stonewall” restrictions, which are related to rotation velocity and volumetric flow limits;
- Usually, pipes in a network system have upper limit and lower limit pressure restrictions. The upper limit is used to prevent accidents that could be a result of excessive pressure conditions. There are also lower limits for pressure in a given system, in order to prevent pressure to decrease to levels that are not economically feasible.

Due to the high level of non-linearity that it involves, this problem needs a large number of calculations and is tackled with search algorithms, also known as metaheuristics. These algorithms use different procedures that basically rely on the same principle: the search for different points within a certain domain of the function in order to find the best outcome as an optimal solution. However, since the function is highly non-linear, the

definition of a global optimum is not guaranteed. Some procedures, such as genetic algorithm, might, at times, converge to a local optimum instead of a global one. Nevertheless, all these search algorithms still may rely on Newton-Raphson iterations, which sometimes may not converge to a solution.

The problem of the fuel cost minimization, as proposed by Wu et al. (2000), also referred to as the classical formulation, is described mathematically in equations 63, 64, 65, and 66, which were slightly modified from the original formulation in order to provide consistency with the methods implemented in this work without deviations from the core ideas behind the original formulation.

Using P-formulation and the nomenclature stated in this work, the problem can be described as follows:

$$\text{Minimize } \sum_{k=1}^{N_s} g_k(q_{gsck}, p_{sk}, p_{dk})$$

*equation 63*

where  $N_s$  is the number of compression stations in the system and  $g_k$  is the fuel consumption function at station  $k$ .

*Subject to:*

$$\sum_{i=1}^N q_{in,i} - \sum_{i=1}^N q_{out,i} + S - D = 0$$

*equation 64*

which enforces nodal material balance. Wu et al. (2001) writes these equations from a different perspective, in  $\Delta P$ -explicit form. In the present work, material balance equations will be treated in Q-explicit form, using the P-formulation of natural gas network analysis, in order to allow for the use of the Linear-Analog method.

Moreover, two other constraints are applied to the system:

$$P_i \in [P^U, P^L]$$

*equation 65*

which accounts for pressure restriction at each node ( $P^U$  = upper pressure limit,  $P^L$  = lower pressure limit). And:

$$P_k \in D_k \quad k = 1, 2, 3, \dots, n_{st}$$

*equation 66*

which accounts for pressure restriction due to “Surge” and “Stonewall” conditions of the compressors according to the compressor domain  $D_k$ , as mentioned in Chapter 3.

## **CHAPTER 5**

### **METHODOLOGY**

This study attempts to address the following problems:

- The estimation of fuel consumption for a given natural gas transportation system;
- The estimation of compressor efficiency;
- The minimization of fuel consumption in a natural gas transportation system.

In order to address these problems, three measures were implemented, respectively:

- By adding fuel consumption to the nodal material balances, it was possible to account for fuel consumption in the system;
- By the use of the compressor efficiency curves presented by Wu et al. (2000), it was possible to estimate efficiencies for a given compressor;
- By the implementation of a domain-constrained search procedure, it was possible to estimate compression station characteristics that will allow minimum gas consumption in a transportation network.

All three approaches were implemented based on a generalized function that used the Linear-Analog method to calculate nodal pressures for a given system.

## 5.1 Fuel Cost Function

It was possible to develop a generalized function that would be able to simulate nodal pressures for a given gas network containing compressors. This generalized function was implemented in Matlab language and named the “fuel cost function”. The fuel cost function was developed with a target of being able to solve different system configurations, including those that comprise compression stations. The function solves the problem in P-formulation and uses the Linear Analog method to solve the system of non-linear equations.

Within the function script, a series of inputs must be specified, such as pipe characteristics, heights, and supplies and demands at each node. Fluid characteristics are also inputs that must be provided. The information on the compressor characteristics must also be provided within the script. Finally, the type of friction factor calculation to be performed is specified: Weymouth, Panhandle-A, Panhandle-B, AGA Fully Turbulent, or Colebrook Formula.

The function collects a vector of compression ratios and outputs the total fuel consumption and the horsepower usage per compressor. If no compression is taking place, then the fuel consumption calculated will be zero. The function also outputs the pressures calculated for each node of the system, flowrate through the compression station, compressor rotation velocity, compressor head and compressor output temperature.

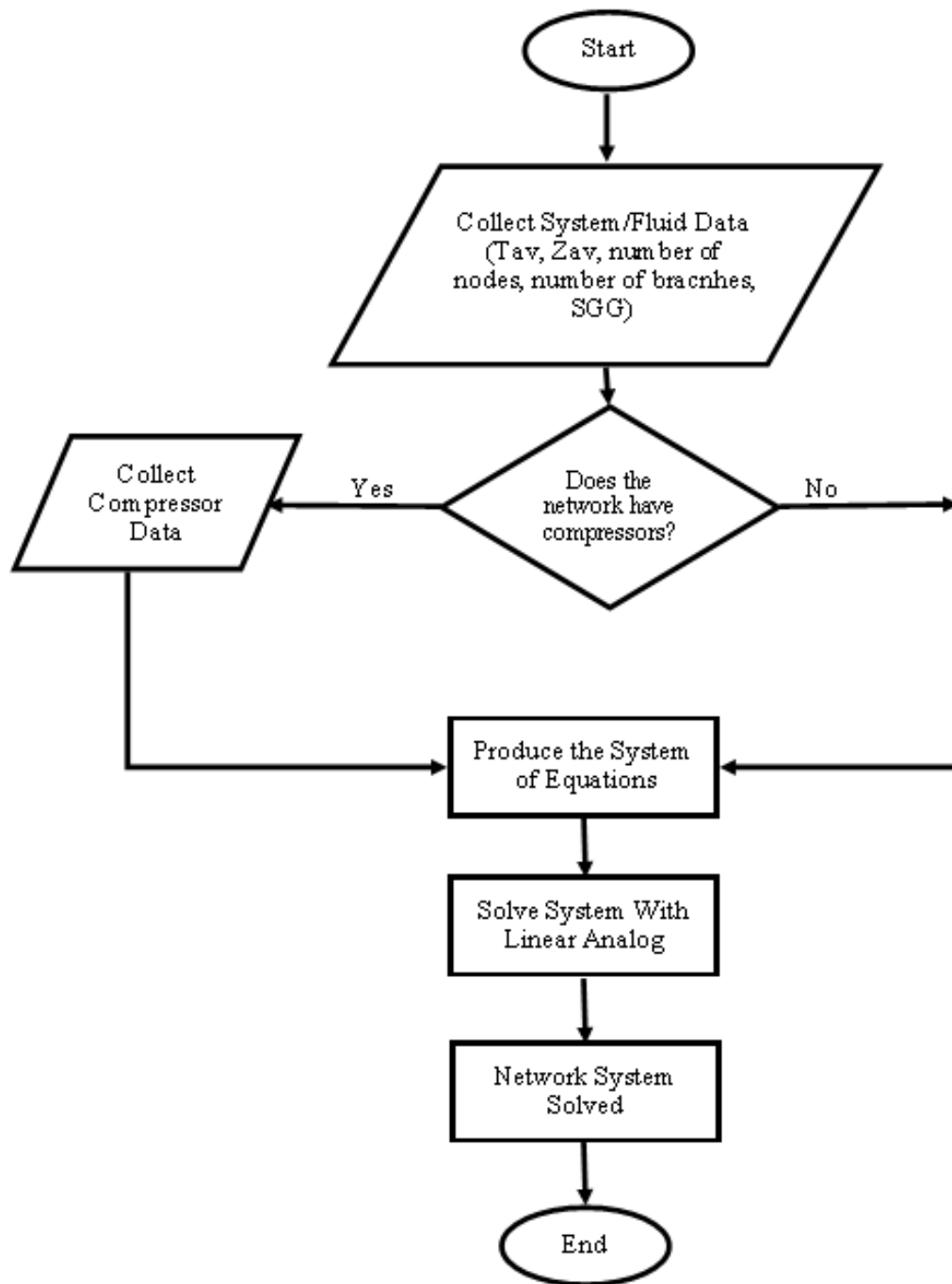


Figure 12: Fuel function algorithm.

## 5.2 The Estimation of Fuel Consumption

Fuel consumption was estimated by the addition of one more element to the material balance performed at the suction node of a compressor. This element corresponds to the amount of horsepower used in the compression station multiplied by the estimated amount of natural gas needed to be burned in order to produce that amount power, which would be:

$$g_k = Cf \left[ \frac{SCFD}{HP} \right] * HP_k[HP]$$

*equation 67*

where:

$g_k$  stands for the fuel consumption in compression station  $k$ .

$Cf$  stands for the consumption factor;

$HP_k$  corresponds to the horsepower usage in compression station  $k$ .

The basis for the consumption factor calculation is on the heat content of the gas, usually given in BTU/SCF according to industry data, and which can be converted to units of HP/SCFD as an estimation of power produced by a certain flow of consumed gas. This term will be present in the characteristic matrix  $\mathbf{K}$  of the Linear Analog method. Figure 15 of Chapter 6 will demonstrate how this term will appear in the system.

### 5.3 The Calculation of Compressor Efficiency

Compressor efficiency was calculated by using the efficiency curve provided by Wu et al. (2000). This estimation for compressor efficiency was applied by updating the efficiency at each new Linear Analog iteration until convergence was achieved for both nodal pressures and efficiency calculations.

### 5.4 The Domain-Constrained Search Procedure

The optimization procedure was based on the development of a code that is capable of testing the fuel cost function, with accountability of gas consumption, for a series of compression ratio combinations. For each set of compression ratios, fuel consumption was analyzed and results stored once verified that a certain set of ratios provided smaller fuel consumption than previous ones analyzed and that the system falls into the constrained domain specified according to equations 65 and 66. Following this process, the combination of compression ratios that provided the best outcome is always selected.

The procedure will keep looking for another optimum that is found within constrained limits until all the desired combinations of compression ratios are analyzed. The procedure also analyzed the output temperature at each compressor, and restricted this output to a certain limit. Figure 13 displays the algorithm used in this optimization procedure.

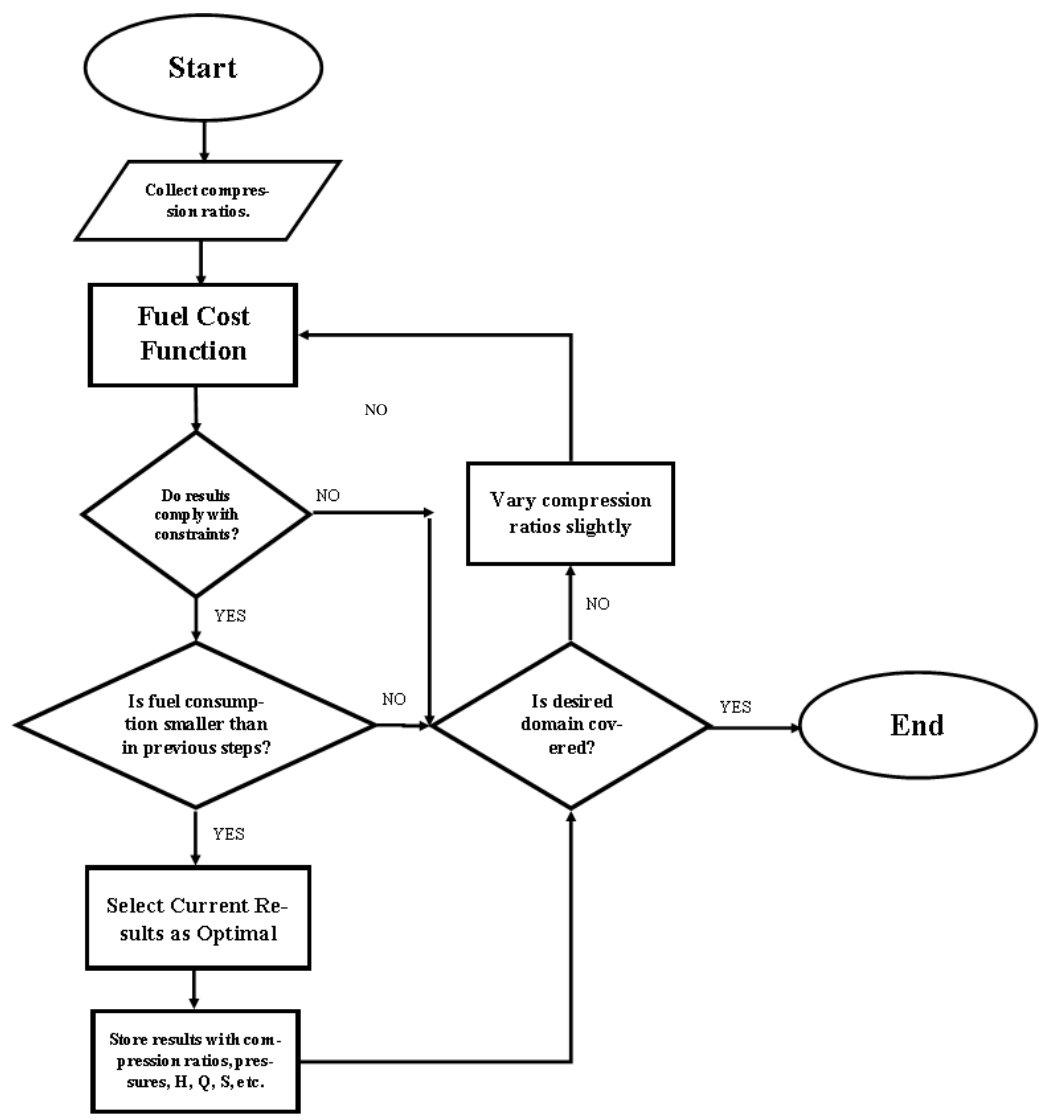


Figure 13: The domain-constrained search procedure

It is important to highlight here that, although this algorithm searches for the optimal solution within a certain constrained domain of the fuel cost function, given a series of system restrictions, the search method implies some limitations, since some factors regarding the minimization problem are not considered in depth:

- First, the fuel cost here estimated is not calculated in the basis of actual currency, but rather in terms of cubic feet of gas per day. Once it is noticeable that the fuel cost is a strong and direct function of gas consumption, perhaps the same could also be said with regards of the feasibility of the application of the domain-constrained search method. In other words, the optimization procedure effectiveness will also depend on fuel price, and not only on fuel consumption, according to the understanding that there might be scenarios in which natural gas price becomes so low, that optimization procedures might become methods whose solution, although sensible from a mathematical perspective, is ineffective in terms of real applications. This is due to the fact that, if gas price is too low; the savings achieved by minimization process might not be enough to justify the implementation of optimization procedure itself;
- Another important topic that is related to the applicability of the model regards the moment of its application in a real case. There are different moments in which optimization could be implemented in a real scenario. It could be performed either during the planning of the network, during the expansion of the network and also during the adjustment of the conditions of a certain system that is already in place. At each one of these stages, the optimization procedure could be implemented in order to plan a new transportation network, to plan the expansion of a network that already exists, or to optimize a network that is not operating under optimal conditions;

- One of the aspects of the cost minimization in natural gas transportation networks also pertains the investment required in order to install the compression station. This investment required is not considered for the effects of this work.

## **CHAPTER 6**

### **RESULTS AND DISCUSSION**

The methodologies proposed in this work were applied to three different cases, each of which focused on a specific aspect of the research conducted.

In Case Study 1, the estimation of fuel consumption was performed in a system composed of 11 nodes and 1 compressor in which compressor efficiency is assumed to be constant.

In Case Study 2, the fuel consumption calculations performed in the system of Case Study 1 were expanded and applied to an analogous system in order to account for the estimation of actual compressor efficiency.

In Case Study 3, a domain-constrained search was implemented in a system composed of 10 nodes and 2 compression stations in order to estimate the combination of compression ratios that would allow minimum fuel consumption in the system.

#### 6.1 Case Study 1

Case Study 1 was based on the system studied by Leong and Ayala (2013). The system is composed of 11 nodes and 1 compression station where a single compressor is present. This system is depicted in Figure 14.

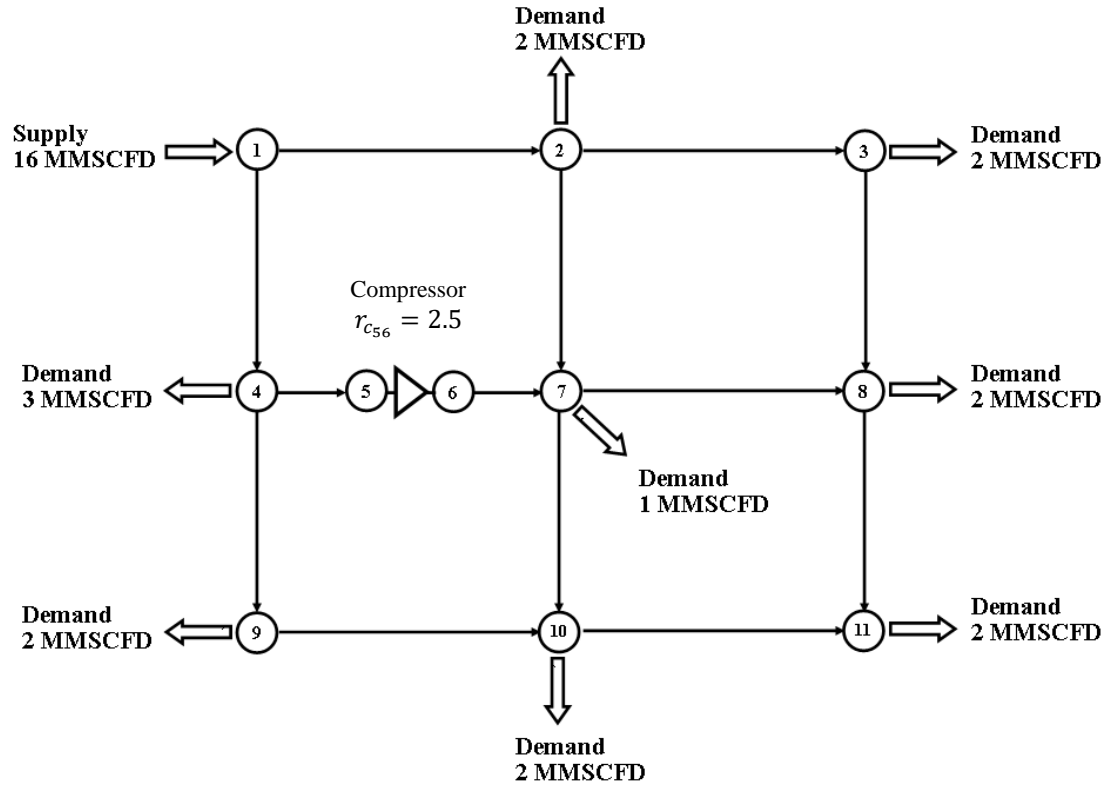


Figure 14: Case Study 1, based on Leong and Ayala (2013).

The fluid properties of the gas in the system are as follows: an average compressibility factor ( $z_{av}$ ) of 0.9 and a gas specific gravity of 0.69. The system is expected to operate at an average temperature of 75 DEG F. Pipe roughness ( $e$ ) is 0.0018 in. Pressure at node 11 is fixed at 130 psi. Compressor efficiency is assumed to be constant at a value of 0.9, and the polytropic coefficient is known to be 1.4. Compression ratio ( $r_{c_{56}}$ ) is 2.5.

In this system, the gas consumption factor ( $Cf$ ) is assumed to be 64 SCFD/HP. This value is based on a gas heat content of 1030 BTU/SCF (US Energy Information

Administration, 2016) and a combustion efficiency of 0.9263 ( $Cf = \frac{61,066.4 \frac{BTU}{D}}{HP} * \frac{1}{1030 \frac{BTU}{SCF}} *$

$\frac{1}{0.9263}$  ). The system is also characterized by inclinations between its different nodes. Table 2 displays the information on the nodal heights. All heights are given by using node 11 as the reference node. Table 3 informs the dimensions of the pipes in the network.

Node	Height (ft)
1	2000
2	800
3	2000
4	1200
5	800
6	800
7	400
8	1600
9	400
10	1000
11	0

Table 2: Height of different nodes of the system.

Branch	Length (miles)	Diameter (in)
(1,2)	30	6.065
(2,3)	30	6.065
(1,4)	30	6.065
(2,7)	30	4.026
(3,8)	30	4.026
(4,5)	15	4.026
(5,6)	Compressor	
(6,7)	15	4.026
(7,8)	30	6.025
(4,9)	30	4.026
(7,10)	30	4.026
(8,11)	30	4.026
(9,10)	30	4.026
(10,11)	30	4.026

Table 3: Dimensions of network pipes.

For this case, the main challenge relies on coupling the expression for fuel consumption to the Linear Analog solution scheme. This is done by accounting for the fuel consumption when performing material balance at node 5, which will cause a slight modification in the Linear Analog characteristic matrix  $\mathbf{K}$ . The Linear-Analog iterations started with an initial guess of  $L_{ij} = \omega * C_{ij}$ , where  $\omega = 1$  in order to follow the same approach implemented by Leong and Ayala (2013).

This matrix will be constructed as follows:

$$\begin{bmatrix} -O_1 & e^{s_{12}/2}L_{12} & 0 & e^{s_{14}/2}L_{14} & 0 & 0 & 0 & 0 & 0 & 0 & 0 \\ L_{12} & -O_2 & e^{s_{23}/2}L_{23} & 0 & 0 & 0 & e^{s_{27}/2}L_{27} & 0 & 0 & 0 & 0 \\ 0 & L_{23} & -O_3 & 0 & 0 & 0 & 0 & e^{s_{38}/2}L_{38} & 0 & 0 & 0 \\ L_{14} & 0 & 0 & -O_4 & e^{s_{45}/2}L_{45} & 0 & 0 & 0 & e^{s_{49}/2}L_{49} & 0 & 0 \\ 0 & 0 & 0 & L_{45} & -O_5 & (-C_{c56} - Cf) & 0 & 0 & 0 & 0 & 0 \\ 0 & 0 & 0 & 0 & -r_{56}L_{67} & C_{c56} & e^{s_{67}/2}L_{67} & 0 & 0 & 0 & 0 \\ 0 & L_{27} & 0 & 0 & r_{56}L_{67} & 0 & -O_7 & e^{s_{78}/2}L_{78} & 0 & e^{s_{7,10}/2}L_{7,10} & 0 \\ 0 & 0 & L_{38} & 0 & 0 & 0 & L_{78} & -O_8 & 0 & 0 & e^{s_{8,11}/2}L_{8,11} \\ 0 & 0 & 0 & L_{49} & 0 & 0 & 0 & 0 & -O_9 & e^{s_{9,10}/2}L_{9,10} & 0 \\ 0 & 0 & 0 & 0 & 0 & 0 & L_{7,10} & 0 & L_{9,10} & -O_{10} & e^{s_{10,11}/2}L_{10,11} \\ 0 & 0 & 0 & 0 & 0 & 0 & 0 & 0 & 0 & 0 & 1 \end{bmatrix} \begin{bmatrix} P_1 \\ P_2 \\ P_3 \\ P_4 \\ P_5 \\ HP \\ P_7 \\ P_8 \\ P_9 \\ P_{10} \\ P_{11} \end{bmatrix} = \begin{bmatrix} -16 \\ 2 \\ 2 \\ 3 \\ 0 \\ 0 \\ 1 \\ 2 \\ 2 \\ 2 \\ 130 \end{bmatrix}$$

Figure 15: Linear analog characteristic matrix with fuel consumption calculation for Case Study 1.

When confronted against Leong and Ayala (2013)'s matrix, the difference is found in the presence of the additional term  $(Cf)$  in row 5, column 6. The matrix can also be rewritten in simplified notation by:

$$\mathbf{K P} = \mathbf{S}$$

For the calculations performed in this case, the method applied used AGA fully turbulent friction factors. The results from the application of the Linear Analog procedure with estimations of fuel consumption are shown in in Figures 16, 17, and 18. In Figure 16, it is demonstrated how nodal pressures converged during Linear Analog iterations. In

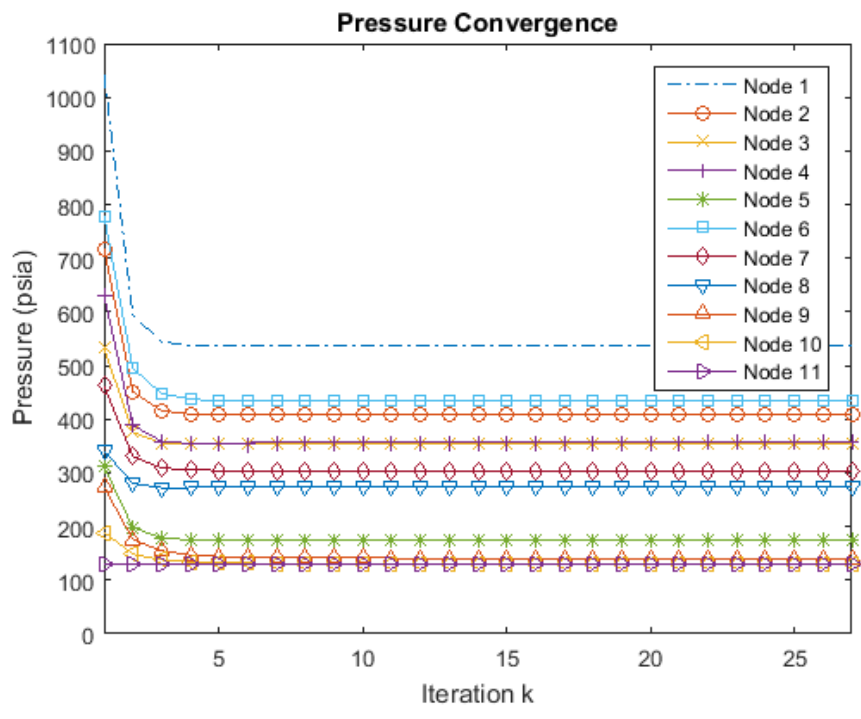


Figure 16: Pressure convergence for Case Study 1.

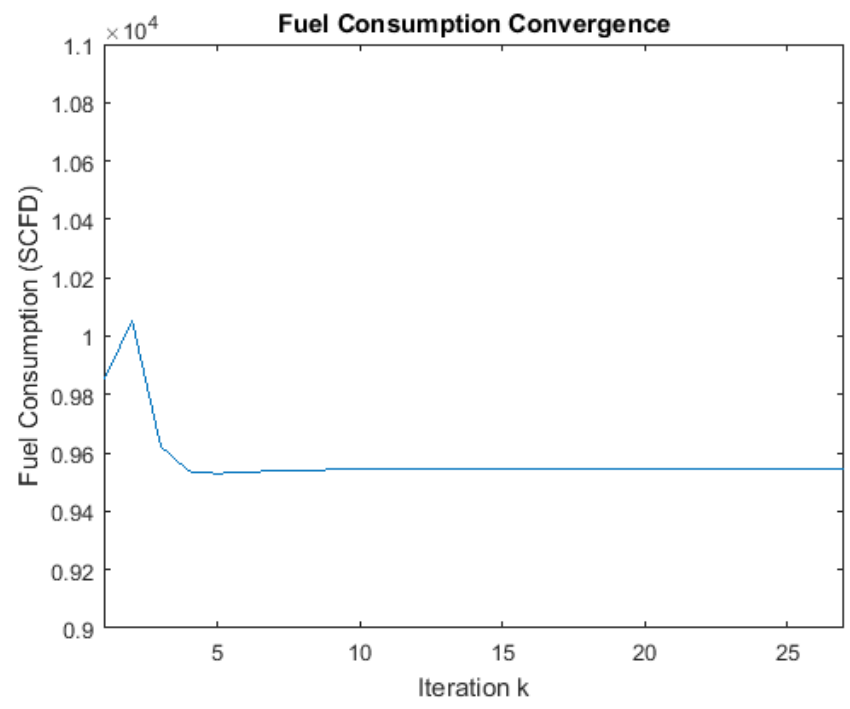


Figure 17: Fuel consumption convergence for Case Study 1.

Figure 17, it is demonstrated how fuel consumption converged during Linear-Analog iterations.

Stop criteria for the iteration scheme was assumed to be  $10^{-12}$  psia. This stop criteria will be adopted in all further developments. In Figure 18, the results for the simulated nodal pressure distribution in the system are displayed.

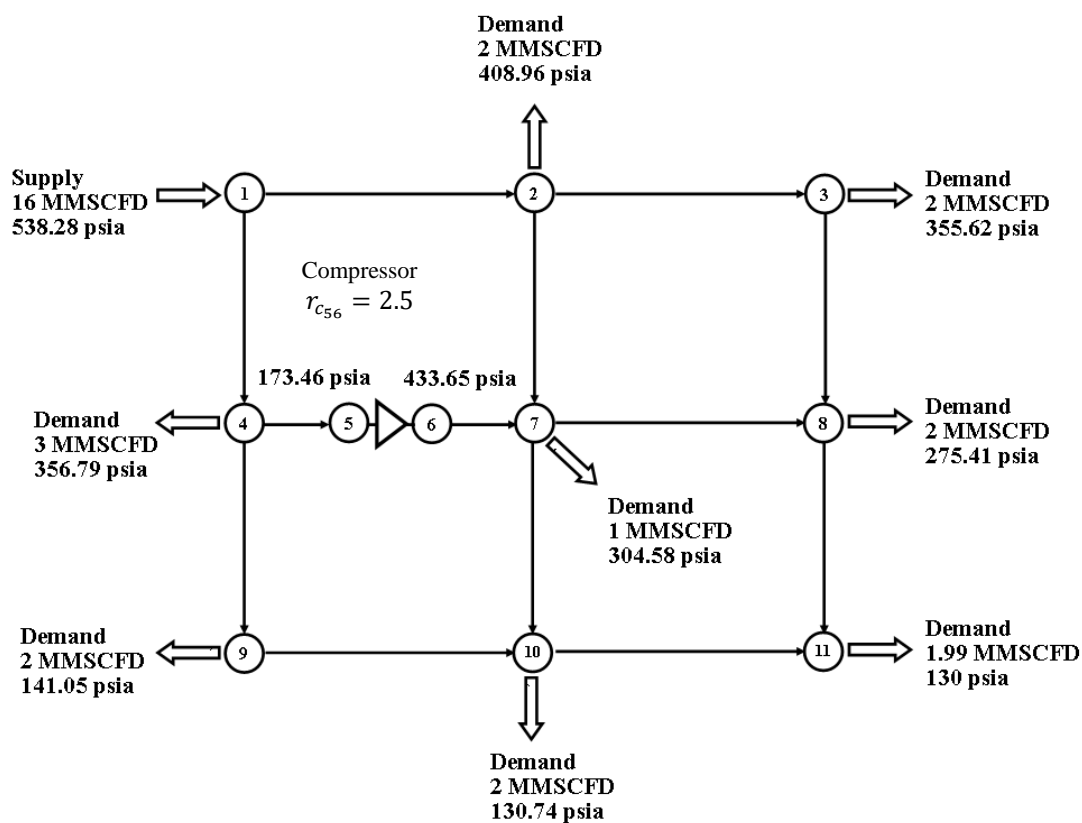


Figure 18: Nodal pressures simulated for Case Study 1.

Final results demonstrated to have a slight variation with respect to those values estimated by Leong and Ayala (2013). The total fuel consumption was estimated to be 9.54 MSCFD. It is important to highlight that, since the system now operates under conditions

in which fuel consumption is taken into consideration, node 11 will not be supplied by 2 MMSCFD, but rather by 1.99 MMSCFD.

## 6.2 Case Study 2

Case Study 2 was based on a natural gas transportation network that is analogous to the system studied by Leong and Ayala (2013). It was performed as an expansion to the procedure presented in Case Study 1, by implementing estimations of actual compressor efficiency, assuming a centrifugal compressor comparable to that studied by Wu et al. (2000).

The system in Case Study 2 is said to be analogous because it is characterized by pipes with larger diameters than those of the pipes studied in Case Study 1. The diameters are modified in order to allow for fluid compression in compression station to be performed between reasonable limits of actual volumetric flow. If pipe diameter is too small, there is a restriction on the actual volumetric flowrate going through the compressor, and lower bounds of volumetric flow will be reached, making it impossible to apply the compressor performance curves as predicted by Wu et al. (2000).

The fluid properties of the gas in the system are also similar to that of Case Study 1: an average compressibility factor ( $z_{av}$ ) of 0.9 and a specific gravity of 0.69. The system is expected to operate at an average temperature of 75 DEG F. Pipe roughness ( $e$ ) is 0.0018 in.

The compression station in the system is also composed of a single compression stage. Compressor coefficient is assumed to have the same value as the polytropic coefficient used by Leong and Ayala (2012) ( $n = n_a = n_p = 1.4$ ) and is the one implemented in the compressor equation presented in chapter 3.

The system in Case Study 2 is also composed of 11 nodes and 1 compression station. This system is depicted in Figure 19.

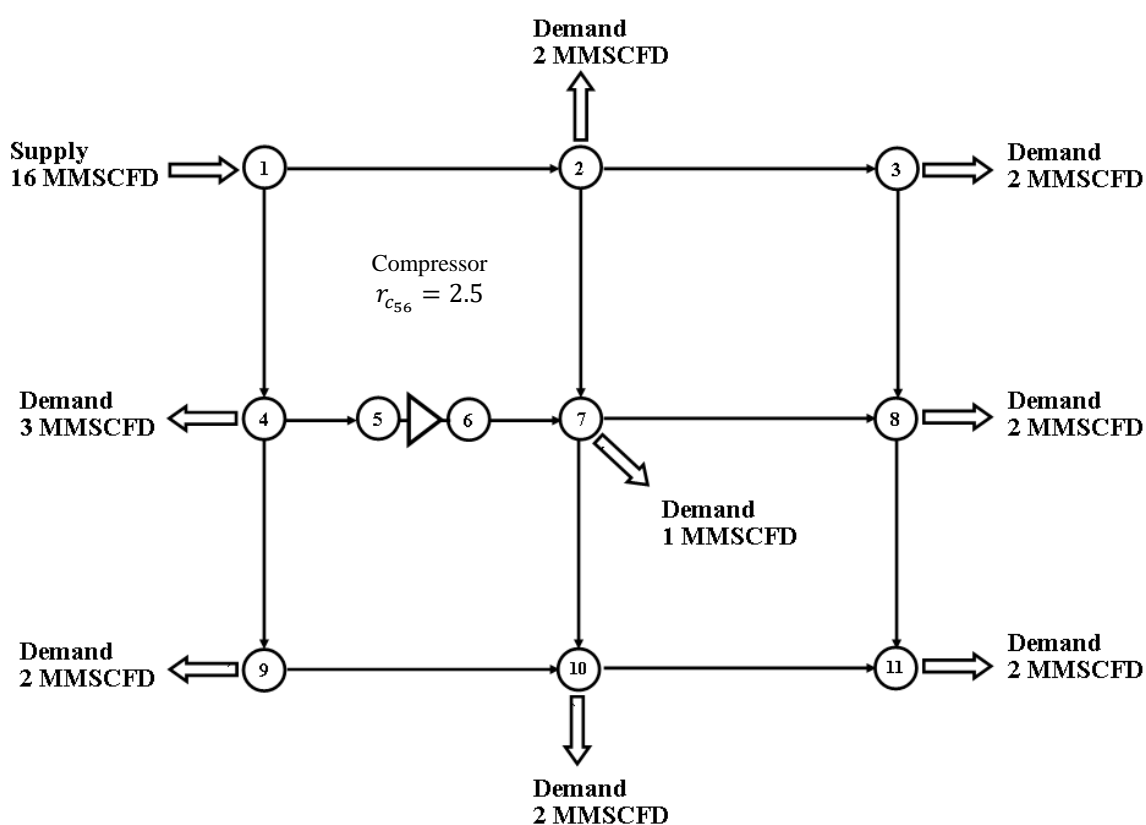


Figure 19: Case Study 2, analogous to Leong and Ayala (2013).

In this system, the gas consumption factor ( $C_f$ ) is also assumed to be 64 SCFD/HP, which is calculated the same way that it is calculated in Case Study 1. The system is characterized by inclinations between its different nodes. Table 4 gives information of

system heights. All heights are given by using node 11 as the reference node. Table 5 informs the dimensions of the network pipes. Note that the dimensions of diameters of the pipes in this case are almost four times higher than those of the pipes used in Case Study

1. Pressure at node 11 is fixed at 500 psia.

Node	Height (ft)
1	2000
2	800
3	2000
4	1200
5	800
6	800
7	400
8	1600
9	400
10	1000
11	0

Table 4: Height of different nodes in the system.

Branch	Length (miles)	Diameter (in)
(1,2)	30	23.6535
(2,3)	30	23.6535
(1,4)	30	23.6535
(2,7)	30	15.7014
(3,8)	30	15.7014
(4,5)	15	15.7014
(5,6)	Compressor	
(6,7)	15	15.7014
(7,8)	30	23.4975
(4,9)	30	15.7014
(7,10)	30	15.7014
(8,11)	30	15.7014
(9,10)	30	15.7014
(10,11)	30	15.7014

Table 5: Dimensions of network pipes.

For this case, the main challenge relies on performing the calculations for efficiency. This is done by updating efficiency at each new Linear Analog iteration, starting from an initial guess of 0.7. Fuel consumption is also accounted for in the Linear Analog solution procedure in the same way it is performed in Case Study 1. This is implemented by performing material balance on node 5, including the fuel that is being consumed, which will also cause a slight modification in the Linear Analog characteristic matrix  $\mathbf{K}$ . This matrix will be constructed according to a system of linear equations formed from nodal material balance:

$$\begin{bmatrix} -O_1 & e^{s_{12}/2}L_{12} & 0 & e^{s_{14}/2}L_{14} & 0 & 0 & 0 & 0 & 0 & 0 & 0 \\ L_{12} & -O_2 & e^{s_{23}/2}L_{23} & 0 & 0 & 0 & e^{s_{27}/2}L_{27} & 0 & 0 & 0 & 0 \\ 0 & L_{23} & -O_3 & 0 & 0 & 0 & 0 & e^{s_{38}/2}L_{38} & 0 & 0 & 0 \\ L_{14} & 0 & 0 & -O_4 & e^{s_{45}/2}L_{45} & 0 & 0 & 0 & e^{s_{49}/2}L_{49} & 0 & 0 \\ 0 & 0 & 0 & L_{45} & -O_5 & (-C_{c56} - Cf) & 0 & 0 & 0 & 0 & 0 \\ 0 & 0 & 0 & 0 & -r_{56}L_{67} & C_{c56} & e^{s_{67}/2}L_{67} & 0 & 0 & 0 & 0 \\ 0 & L_{27} & 0 & 0 & r_{56}L_{67} & 0 & -O_7 & e^{s_{78}/2}L_{78} & 0 & e^{s_{7,10}/2}L_{7,10} & 0 \\ 0 & 0 & L_{38} & 0 & 0 & 0 & L_{78} & -O_8 & 0 & 0 & e^{s_{8,11}/2}L_{8,11} \\ 0 & 0 & 0 & L_{49} & 0 & 0 & 0 & 0 & -O_9 & e^{s_{9,10}/2}L_{9,10} & 0 \\ 0 & 0 & 0 & 0 & 0 & 0 & L_{7,10} & 0 & L_{9,10} & -O_{10} & e^{s_{10,11}/2}L_{10,11} \\ 0 & 0 & 0 & 0 & 0 & 0 & 0 & 0 & 0 & 0 & 1 \end{bmatrix} \begin{bmatrix} P_1 \\ P_2 \\ P_3 \\ P_4 \\ P_5 \\ HP \\ P_7 \\ P_8 \\ P_9 \\ P_{10} \\ P_{11} \end{bmatrix} = \begin{bmatrix} -16 \\ 2 \\ 2 \\ 3 \\ 0 \\ 0 \\ 1 \\ 2 \\ 2 \\ 2 \\ 500 \end{bmatrix}$$

Figure 20: Linear-Analog characteristic matrix with fuel consumption calculation for Case Study 2.

The system can also be rewritten in simplified notation by:

$$\mathbf{K} \mathbf{P} = \mathbf{S}$$

The method applied used AGA fully turbulent friction factor calculations. The results from the application of the Linear Analog procedure to this case are shown in Figures 21-27. In Figure 21, it is demonstrated how pressures converged during Linear-Analog iterations.

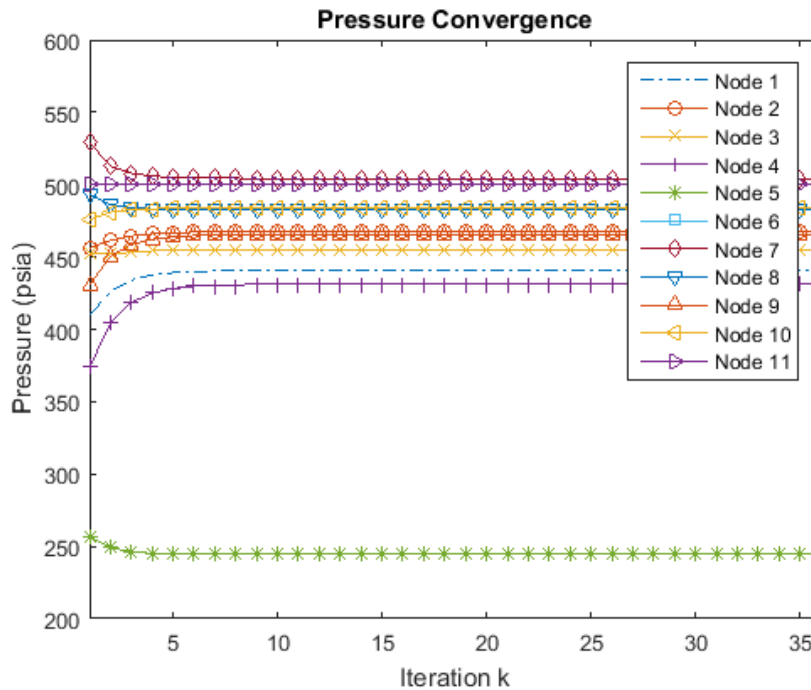


Figure 21: Pressure convergence for Case Study 2.

It can be observed that, despite the inclusion of the calculation of compressor efficiency by the implementation of a very non-linear polynomial equation, the Linear Analog method demonstrates to converge steadily.

It might be inquired the reason why node 5 operates at a pressure condition much lower than that of the other nodes in the system. The explanation for that occurrence relies precisely on the fact that node 5 is the inlet node of the compressor.

In Figure 22, it is shown the convergence of the estimation for efficiency at each Linear Analog iteration after the initial guess. Efficiency value is demonstrated to converge steadily to 0.911, a high efficiency value.

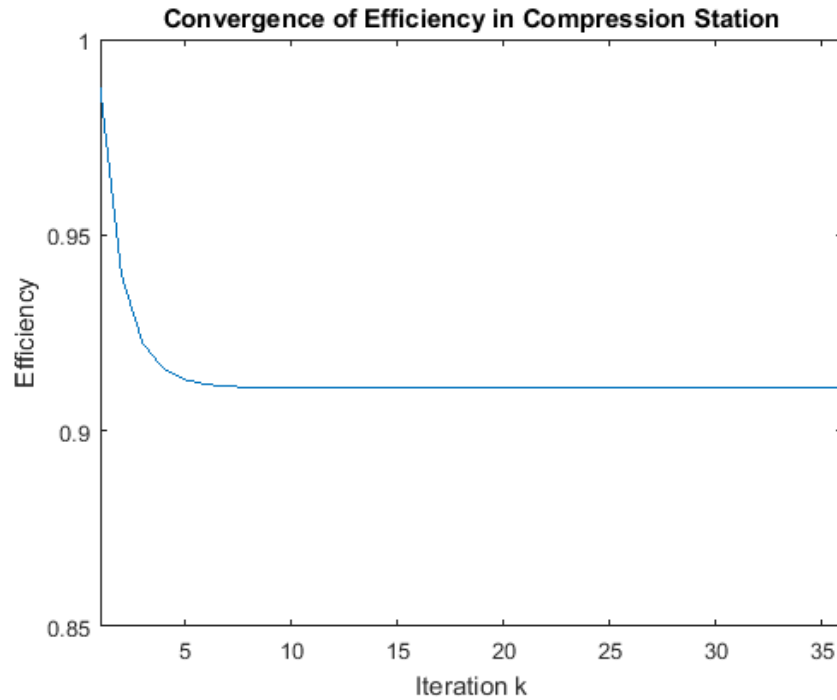


Figure 22: Efficiency convergence for Case Study 2.

In Figure 23, rotation velocity in compressor is also demonstrated to converge accordingly during Linear Analog iterations. This value is given in units of rpm (rotations per minute). In Figure 24, the estimated value of the volumetric flow at standard conditions moving through the compressor is also demonstrated to converge steadily. Figures 25 and 26 also display a convergence scenario during Linear Analog iterations for the estimations of fuel consumption and horsepower usage.

An important observation relies on the fact that, since there is more volumetric flow being compressed in this case, once larger pipes allow for such occurrence, horsepower usage and fuel consumption become much higher than they are in Case Study 1.

Finally, Figure 27 displays nodal pressure distribution within the system, demonstrating how flow is supplied to or demanded by the different nodes of the network.

It is noticeable that, for this case, pressure distribution displays a different pattern than that of pressure distribution simulation achieved in Case Study 1, which is a direct result of the greater impacts of gravitational forces due to inclinations operating in the system and larger flows moving through the pipelines.

As mentioned, since horsepower usage in Case Study 2 was higher, fuel consumption was also estimated to be higher than that of Case Study 1, at a rate of 0.37 MMSCFD.

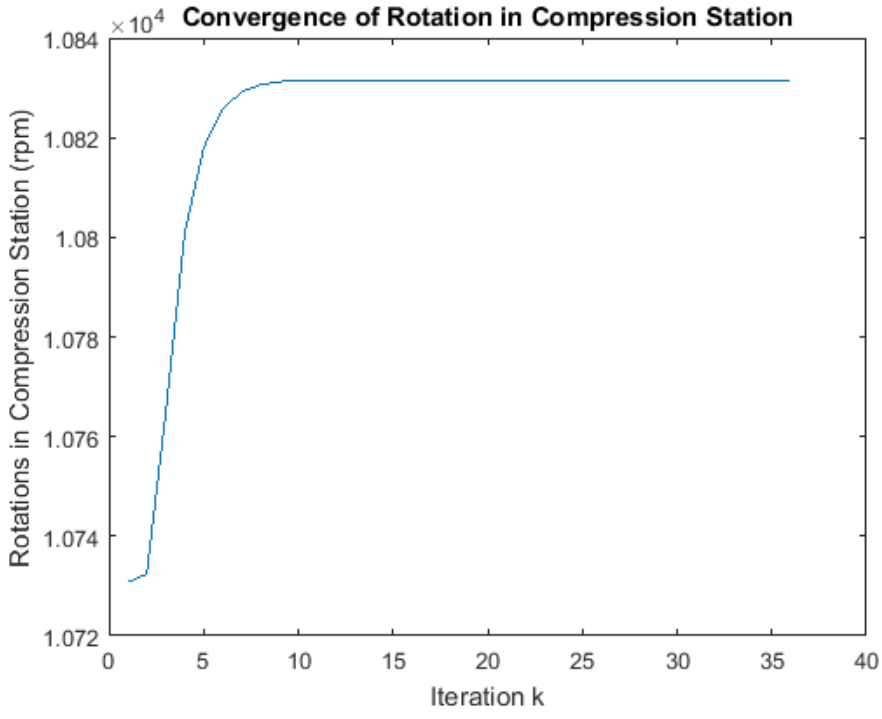


Figure 23: Compressor rotation velocity convergence for Case Study 2.

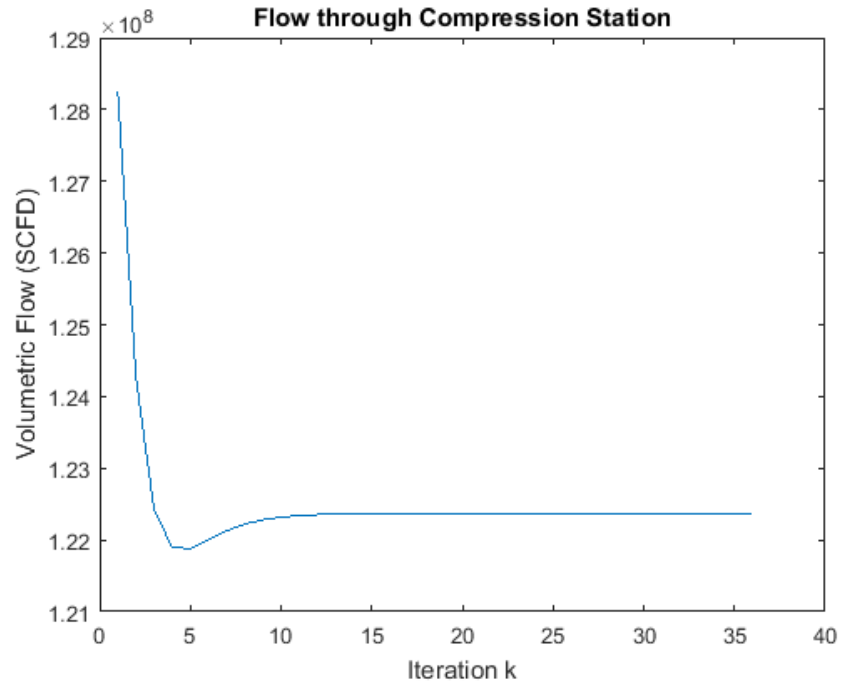


Figure 24: Flow moving through compression station for Case Study 2.

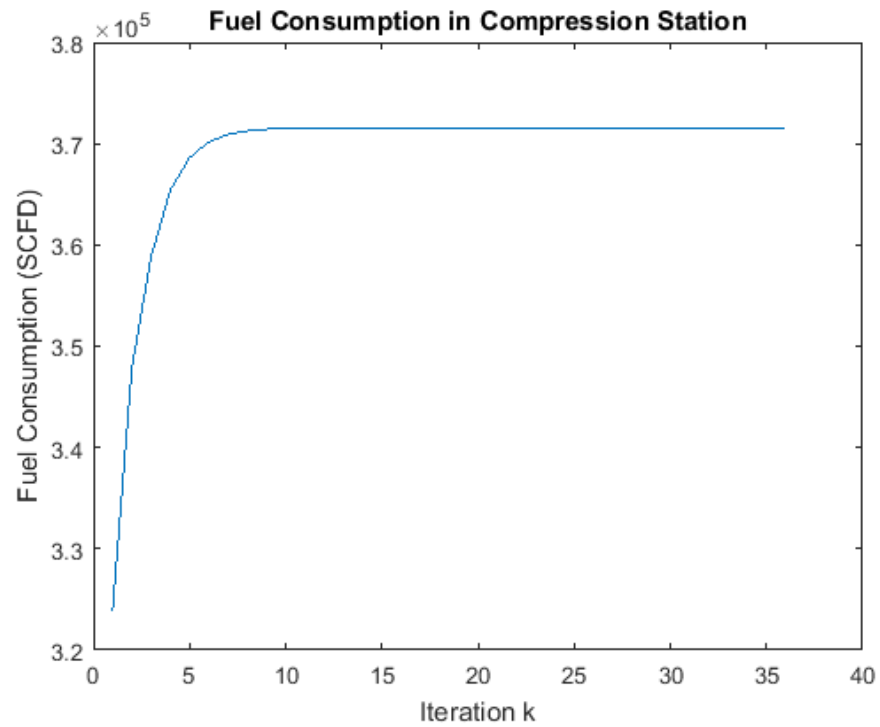


Figure 25: Fuel consumption convergence for Case Study 2.

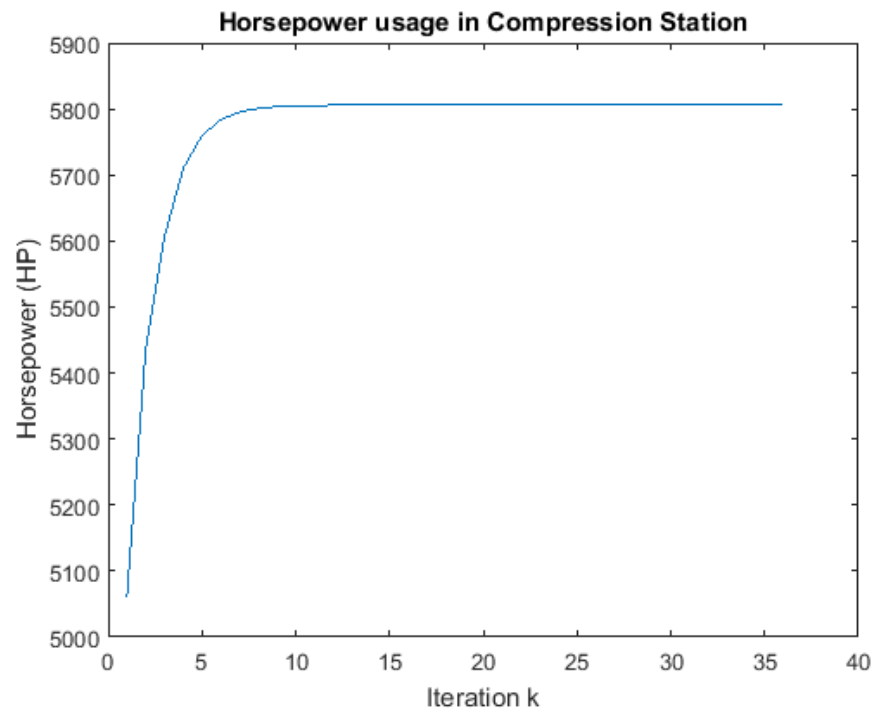


Figure 26: Horsepower usage convergence for Case Study 2.

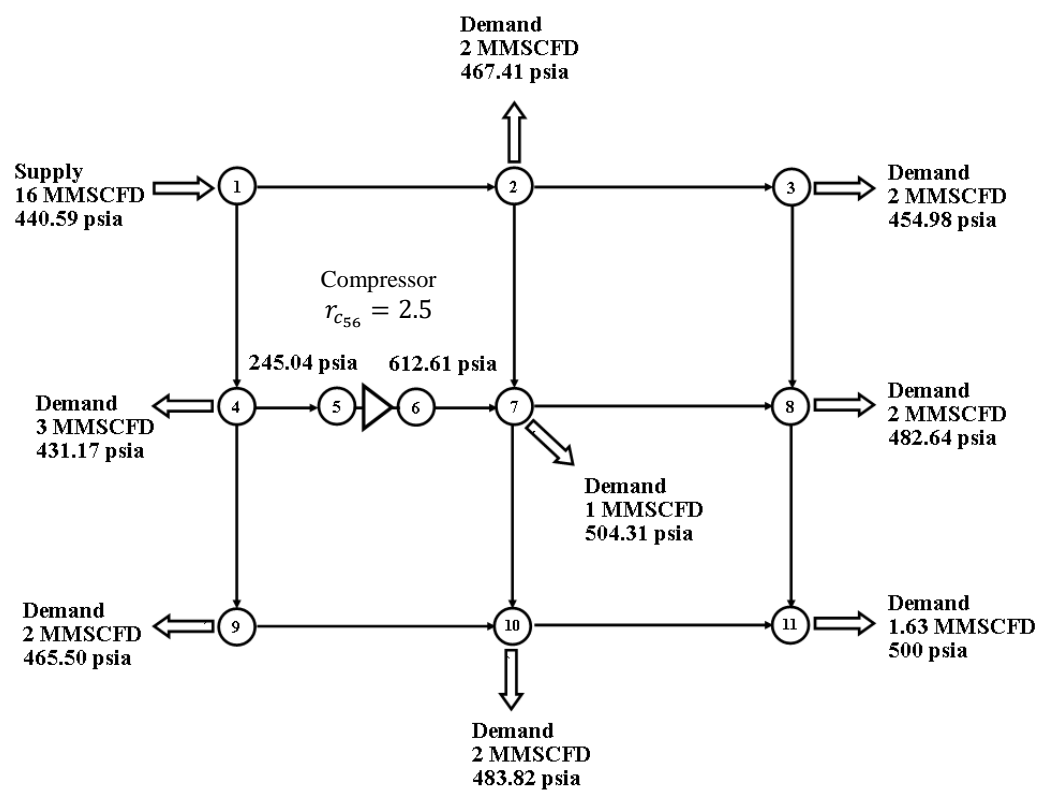


Figure 27: Nodal pressures simulated for Case Study 2.

### 6.3 Case Study 3

Case Study 3 was based on the system studied by Wu et al. (2000), but modified in order to include a loop within the network. In this case, the domain-constrained search method was implemented in order to perform the minimization of fuel consumption in the natural gas transportation network. Yet, the estimations of compressor efficiency and fuel cost were performed in the same way as observed in Case Study 2. The system in Case Study 3 is composed of 10 nodes and 2 compression stations where compression is implemented in two stages. This system is depicted on Figure 28.

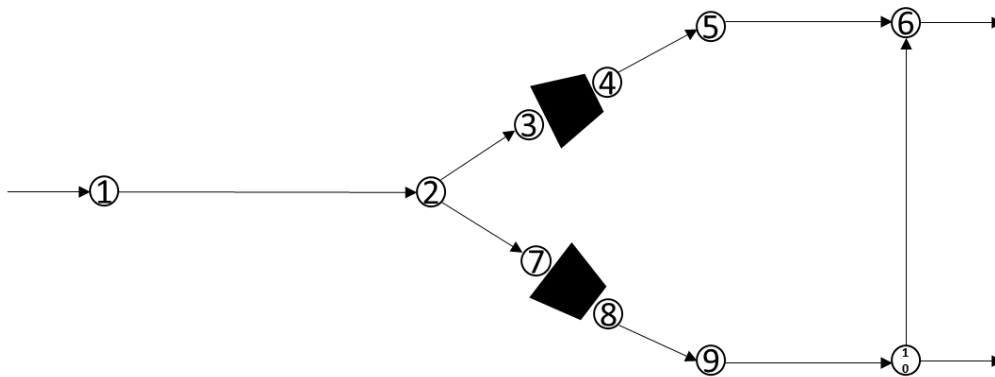


Figure 28: Case Study 3, analogous to Wu et al. (2000), but with the inclusion of a loop.

The fluid properties of the gas in the system are as follows: an average compressibility factor ( $z_{av}$ ) of 0.95 and a specific gravity of 0.6248. The system is expected to operate at an average temperature of 60 DEG F. Pipe roughness ( $e$ ) is 0.0018 in.

Compressor efficiency is initialized at a value of 0.85, and the compressor coefficient is known to be 1.287 ( $n = n_a = n_p = 1.287$ ). Compression ratios ( $r_{c_{34}}, r_{c_{78}}$ ) are

variable and will be evaluated for a range of values for each compression station according to the domain-constrained search protocol. The range of the compression ratio values for such evaluation will vary from 1 to 5.

As mentioned previously, in Case Study 3, the domain-constrained search method will look for the best combination of compression ratios that will make it possible to minimize fuel consumption in the system.

Consumption factor ( $C_f$ ) is also assumed to be 64 SCFD/HP, given the same assumptions on heat content and gas combustion discussed in Case Study 1. The network is not characterized by inclinations between its different nodes.

Table 6 informs the dimensions of the network pipes, and Table 7 informs the characteristics of the compression stations.

It should be noted that the pipes for this case are large since they will handle a high amount of volumetric flow and are designed to be similar to the pipes used in the case studied by Wu et al. (2000).

There is one supply node in the network: node 1. There are also two demand nodes: nodes 6 and 10. It is assumed that only node 10 has a fixed demand of 350 MMSCFD. Node 1 and node 6, however, have specified pressures of 4500 psi and 800 psi, respectively. Since they have specified pressures, the flow entering through node 1 and the flow leaving through node 6 will have values that depend on system conditions, compression ratios used in the compression stations, and fuel consumption in the system.

Branch	Length (miles)	Diameter (in)
(1,2)	450	36
(2,3)	50	36
(4,5)	50	36
(5,6)	50	36
(2,7)	50	36
(8,9)	50	36
(9,10)	50	36
(10,6)	50	36

Table 6: Dimensions of network pipes.

Compressor Characteristics	Compression Station 1	Compression Station 2
Branch	(3,4)	(7,8)
Number of stages	2	2
Compressor coefficient	1.287	1.287
Inlet temperature (DEG F)	80	80
$Z_{av}$	0.89	0.89

Table 7: Characteristics of the compression stations.

In order to explain the practical use of the domain-constrained search method, Case Study 3 will be solved for a series of constraints slightly different from each other. At each new step, a different constraint will be applied to the system, or a new constraint will be added to the constraints already in place. A surface of the constrained domain will be displayed for each one of the steps in order to illustrate how the search surface is reduced as more constraints are added to the system.

### 6.3.1 Case Study 3.a: only fixed pressures at nodes 1 and 6

In the first approach, the system is analyzed for pressure determinations only at nodes 1 and 6, in which pressures are fixed and present the same behavior in all variations of Case Study 3. No other restrictions due to pipe mechanical resistance or compressor conditions are considered.

The surface that is created by analyzing the system fuel consumption for a series of compression ratios is displayed in Figures 29 and 30, which show the same surface from different perspectives. It can be observed that the imposed constraints on nodes 1 and 6 allow for a trivial solution for the optimization problem, where the compression ratios could be assumed to be 1, which informs that no compression would be taking place at all. Once more constraints are added to the system though, it will be observed that the trivial solution will not satisfy the desired restrictions.

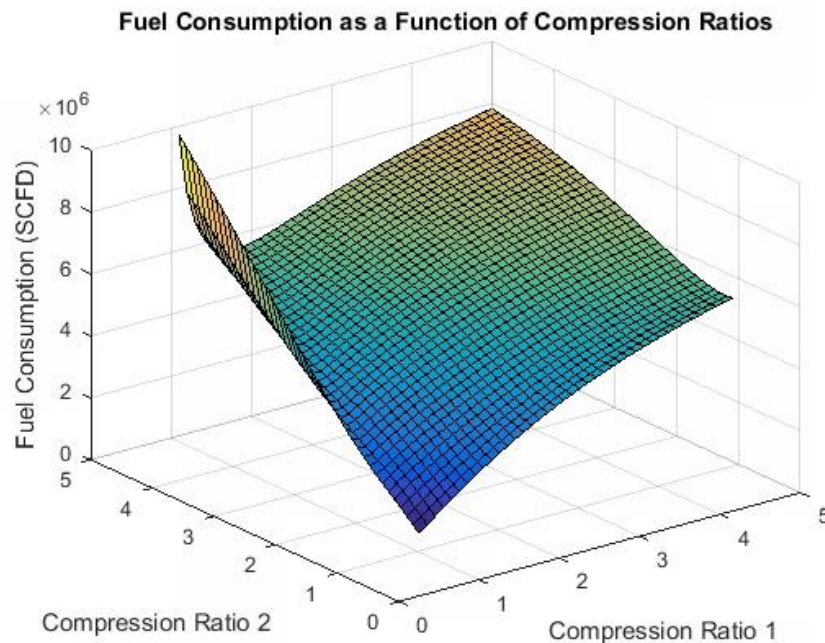


Figure 29: Case Study 3.a: analogous to Wu et al. (2000).

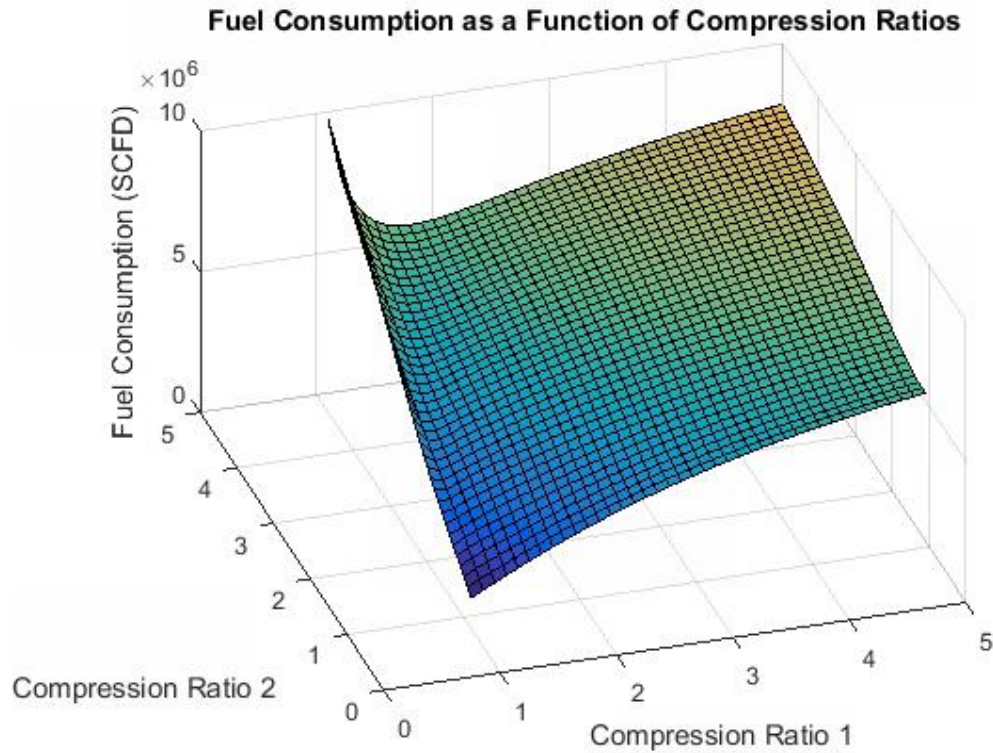


Figure 30: Case Study 3.a: analogous to Wu et al. (2000).

6.3.2 Case Study 3.b: pressure in node 10 is constrained to be higher than 850 psi.

Case Study 3.b applies a new restriction to the system in which it is determined that delivery pressure at node 10 is required to be higher than 850 psi.

This hypothetical scenario is consistent with restrictions observed in the industry since one of the main reasons to have a compression station in a gas transportation pipeline network is the need to guarantee a certain delivery pressure for the further stages in other networks to which the system being studied is connected or delivers gas.

It is noticeable that for such conditions, there is a series of combinations of compression ratios that will not satisfy the imposed constraint and not allow system to deliver gas at node 10 as per the 850 psi.

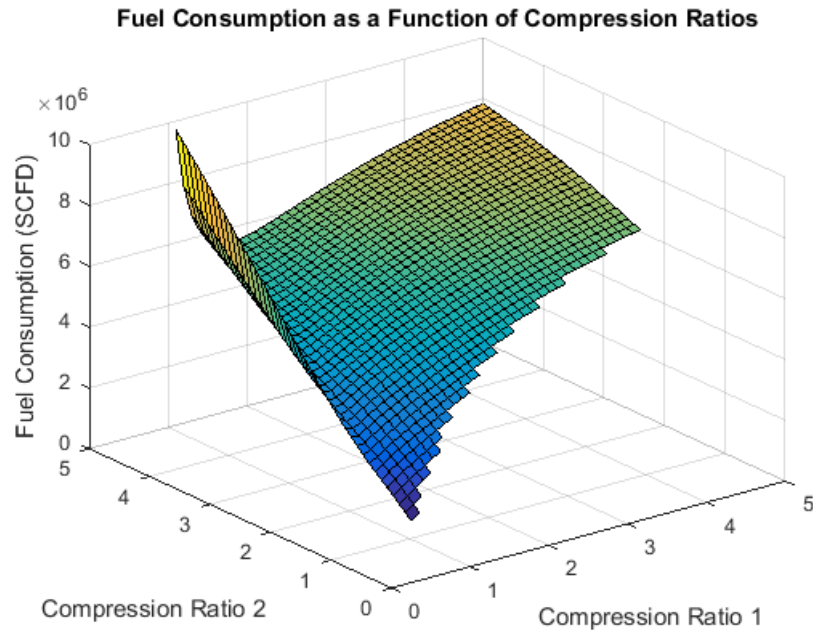


Figure 31: Case Study 3.b: analogous to Wu et al. (2000).

6.3.3 Case Study 3.c, pressure in node 10 is constrained to be higher than 880 psia.

Case Study 3.c applies a new restriction to the system in which it is determined that delivery pressure at node 10 is required to be higher than 880 psi. It is noticeable that for such conditions, there is a larger series of combinations of compression ratios that will not satisfy the imposed constraint and not allow the system to deliver gas at node 10 as per the 880 psi.

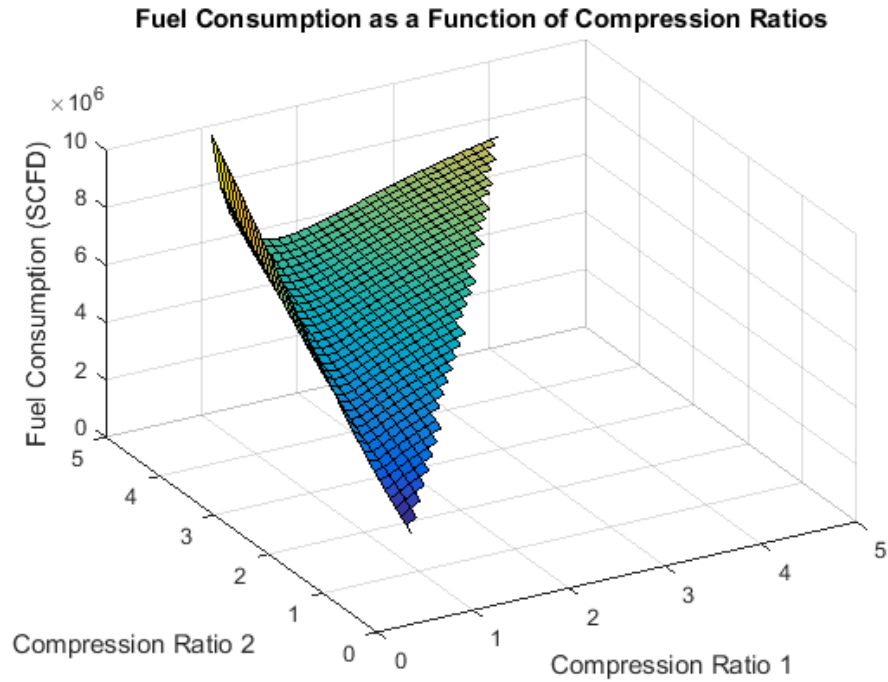


Figure 32: Case Study 3.c: analogous to Wu et al. (2000).

6.3.4 Case Study 3.d, pressure in node 10 is constrained to be higher than 900 psi.

Case Study 3.d applies a new restriction to the system, in which it is determined that delivery pressure at node 10 is required to be higher than 900 psi. It is noticeable that for such conditions, there is an even larger series of combinations of compression ratios that will not satisfy the imposed constraint and not allow the system to deliver gas at node 10 as per the 900 psi.

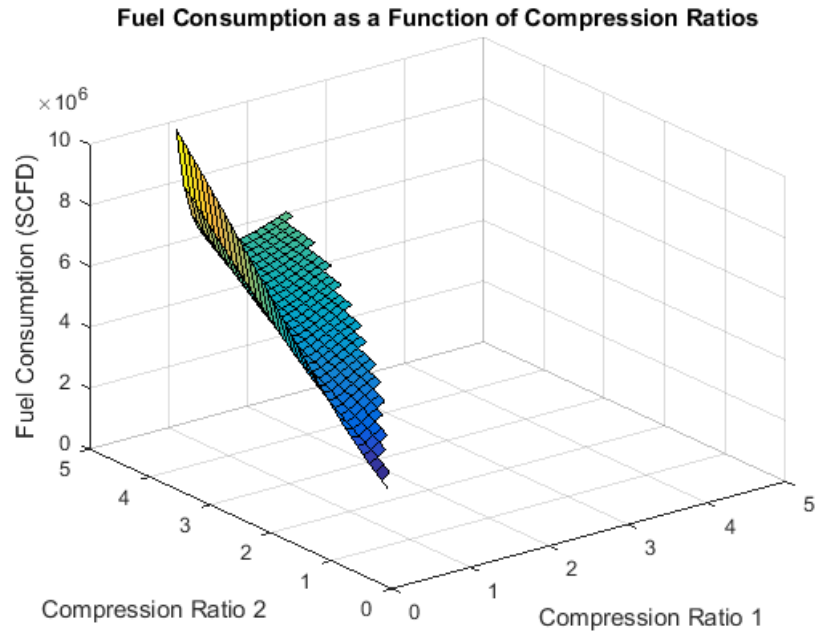


Figure 33: Case Study 3.d: analogous to Wu et al. (2000).

### 6.3.5 Case Study 3.e: constraints in pressure delivery, Surge and Stonewall conditions

Case Study 3.e applies the same restriction according to which it is determined that delivery pressure at node 10 is required to be higher than 900 psi. It is noticeable that for such conditions, the combinations of compression ratios that will not satisfy the imposed constraint and not allow the system to deliver gas at node 10 as per the 900 psi is the same as in variation d of Case Study 3. However, “Surge” and “Stonewall” restriction are now implemented.

It is also assumed that the compression stations are, hypothetically, characterized by:

- Rotation velocities in compressors expected to be greater than 5000 rpm and smaller than 12000 rpm;
- Actual volumetric flow is constrained to be smaller than 27000 ft<sup>3</sup> and higher than 5000 ft<sup>3</sup>.

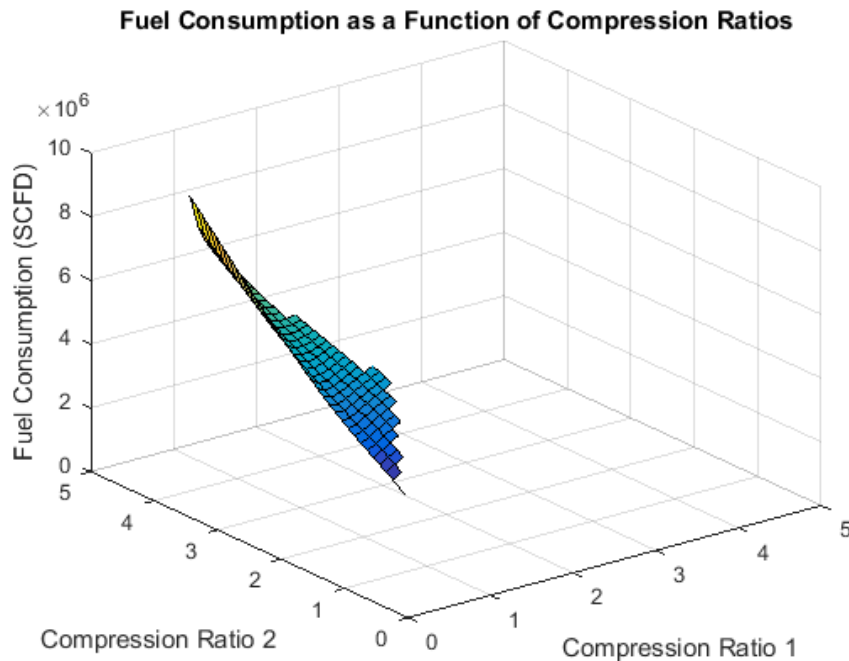


Figure 34: Case Study 3.e: analogous to Wu et al. (2000).

6.3.6 Case Study 3.f: constraints in pressure delivery, Surge conditions, Stonewall conditions, mechanical restrictions, output temperature and pressure at inlet node of compression station 2.

Case Study 3.f applies a new restriction to the system, in which it is determined that delivery pressure at node 10 is required to be higher than 900 psi. Hypothetically, pressure in node 7 is constrained to be lower than 400 psi. It is also assumed that the compression stations are, hypothetically, characterized by:

- Rotation velocities in compressors expected to be greater than 5000 rpm and smaller than 12000 rpm;
- Actual volumetric flow is constrained to be smaller than 27000 ft<sup>3</sup> and higher than 5000 ft<sup>3</sup>;
- All compressor output temperatures are lower than 540 DEG F.

It is also assumed that all nodal pressures are higher than 250 psi and lower than 5000 psi.

Figures 35 and 36 demonstrated how the search domain is restricted. Within this surface, after all constraints are applied, the combination of compression ratios that will allow for minimum fuel consumption will be selected.

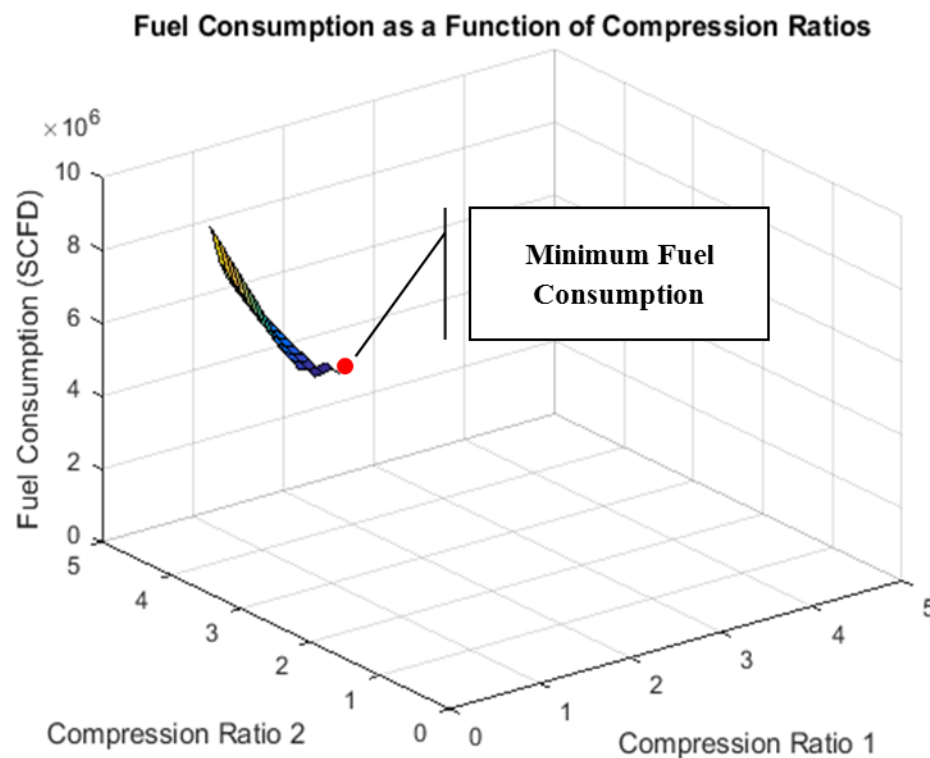


Figure 35: Case Study 3.f: analogous to Wu et al. (2000).

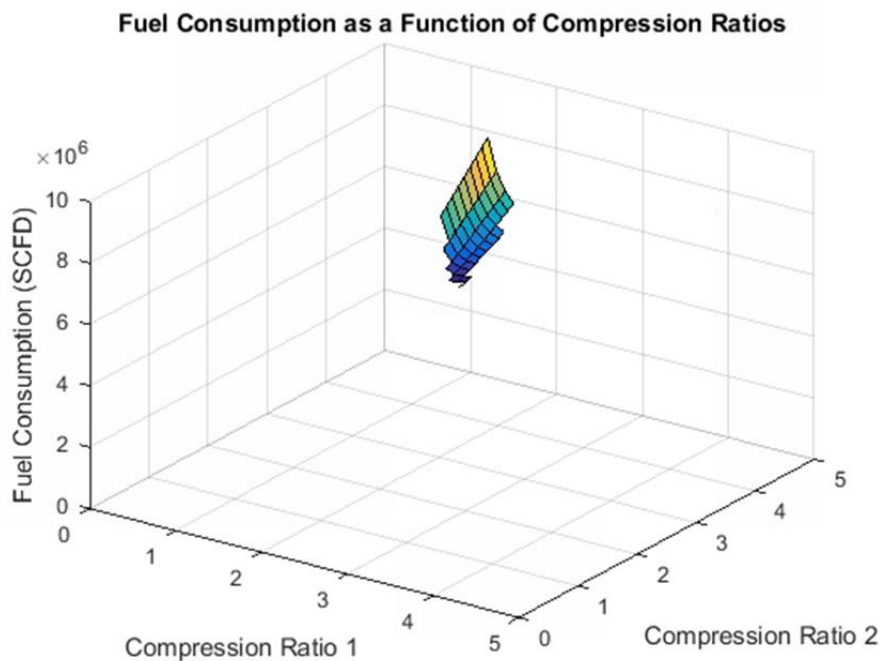


Figure 36: Case Study 3.f: analogous to Wu et al. (2000).

Node	Pressure (psi)
1	4500.00
2	965.44
3	767.31
4	1150.97
5	991.14
6	800.00
7	398.97
8	1556.00
9	1286.56
10	943.06

Table 8: Optimal pressure distribution for Case Study 3.

Fuel consumption in system is estimated to be 4.47 MMSCFD, while optimal compression ratios are found to be 1.5 for compression station 1, and 3.9 for compression station 2. Table 8 informs final pressure distribution within the optimized system.

## **CHAPTER 7**

### **CONCLUDING REMARKS**

The objective of the work here presented was to expand the simulation of natural gas transportation networks in order to account for:

- Fuel consumption in a natural gas transportation network;
- The estimation of compressor efficiency from compressor performance curves and;
- The implementation of the minimization of fuel consumption in a gas network by the manipulation of compression ratios of the compressors in the system, given the system's restrictions. This protocol was named the domain-constrained search method.

All these objectives were achieved successfully with the use of the Linear-Pressure Analog method.

The fuel consumption was estimated within the Linear Analog protocol, as well as the actual compressor efficiency. Finally, it was also possible to demonstrate that the Linear-Pressure Analog is a powerful tool to be implemented in the optimization problems that concern the minimization of fuel consumption in natural gas transportation systems. The relatively good assurance of convergence of the Linear Analog procedure allowed for the test of different scenarios of compression ratios, with selection of the scenario that yielded the best outcome as the optimal case. Thus, the domain-constrained search method

demonstrated to work properly, searching for an optimal value within desired domain. However, it is predicted to demand great computational effort as the number of compression stations and the size of a given system increase.

### 7.1 Future Work

One of the possibilities for future work in the use of the Linear Analog scheme in the optimization of natural gas transportation is that the method allows for a partially linearized system of linear equations. This partial linearization is due to the use of the Linear Analog method as a technique to linearize the gas flow equations in network analysis, which is achieved from the nodal material balance equations written in terms of  $L_{ij}$ . This is performed while keeping the objective function as the original highly non-linear function that is given by compressor horsepower usage multiplied by the consumption factor.

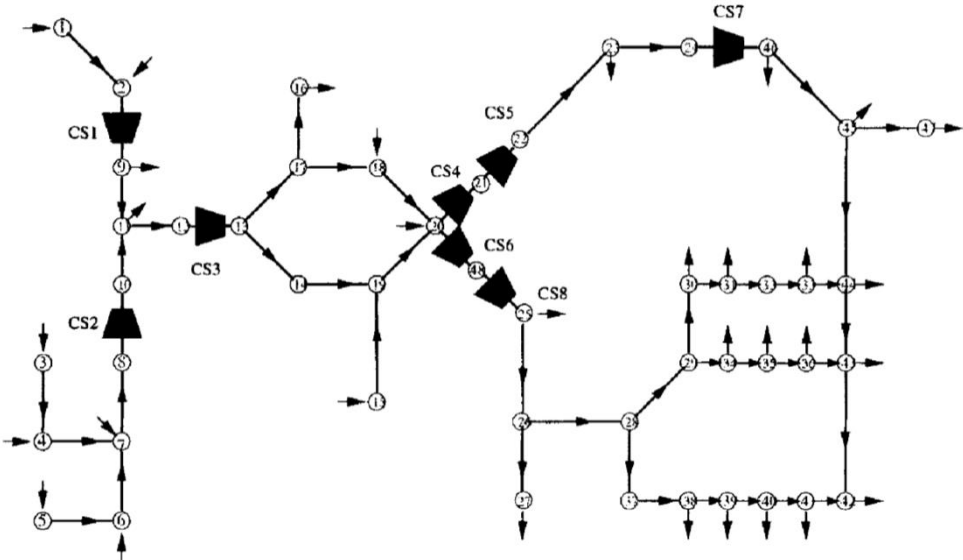


Figure 37: Large natural gas transportation system. Source: Wu et al. (2000).

In order to achieve full linearization, perhaps the objective function can be linearized by a polynomial approximation as performed by Wu et al. (2000). This could allow for the use of Linear Programming in order to solve for the minimization of fuel consumption in natural gas networks.

Furthermore, the domain-constrained search method could be tested for a larger system containing more compression stations, nodes and pipes. A suggestion for this further attempt is found on the case study 3 of Wu et al. (2000), depicted on Figure 37, which performs optimization on a gas transportation network containing 43 pipe branches and 8 compression stations.

## BIBLIOGRAPHY

- AGA-American Gas Association (1965). *Steady Flow in Gas Pipelines: Testing/Masurement/Behavior/Computation*, Institute of Gas Technology Technical Report 10, New York.
- Ayala, L. F. (2012). Chapter 21: Transportation of Crude Oil, Natural Gas, and Petroleum Products. *ASTM Handbook of Petroleum and Natural Gas Refining and Processing*. ASTM International.
- Block, H. P. (1933) *A practical guide to compressor technology*. 2<sup>nd</sup> ed., Hoboken, NJ: John Wiley & Sons.
- Boyd, O. W. (1983). *Petroleum Fluid Systems*, Campbell Petroleum Series, Norman, OK.
- Brill, J. P., and Mukherjee, H. (1999). *Multiphase flow in Wells*, SPE Monograph, Vol. 17, Henry L. Doherty Series, Richardson, TX.
- Brown, R. N. (2005). *Compressors: selection and sizing*. 3<sup>rd</sup> ed., Houston, TX: Elsevier.
- Caterpillar Company (2016). Centrifugal Gas Compressor. [Online image]. Retrieved January 28, 2016 from <http://www.directindustry.com/>
- Cross, H. (1932). *Analysis of Continuous Frames by Distributing Fixed-End Moments*. Transactions of ASCE, v 96, n 1793, 1-10.
- Dranchuk, P. M., and Abou-Kassem, J. H. (1975). *Calculation of Z Factors For Natural Gases Using Equations of State*. Journal of Canadian Petroleum Technology, 3436.
- Ferguson, J.W. (1936). *A Mathematical Analysis of the Effect of Differences on Flow Formulae for Gas Pipes*, Gas Age, Vol. 78, pp. 72-76.
- GPSA, Gas Processors Suppliers Association (2004), *Fluid Flow and Piping*. GPSA Engineering Data Book, 12<sup>th</sup> ed., Tulsa, OK: Gas Processors Association.
- Gresh, M T., (2001). *Compressor Performance: Aerodynamics for the User*. 2<sup>nd</sup> ed. Woburn, MA: Butterworth-Heinemann.
- Ikoku, C. U. (1984). *Natural Gas Production Engineering*. New York: John Wiley and Sons.
- Johnson, T. W., and Berwald, W. B. (1935). *Flow of Natural Gas Through High Pressure Transmission Lines*. U.S. Department of the Interior Bureau of Mines.

- Larock, B. E., Jeppson, R. W., and Watters, G. Z. (1999). *Hydraulics of Pipeline Systems*.
- Lee, A., Gonzalez, M., Eakin, B. (1966), *The Viscosity of Natural Gases*, SPE Paper 1340, Journal of Petroleum Technology, vol. 18, p. 997-1000. CRC Press.
- Leong, Y. C. and Ayala, L. F. (2012). *A robust linear-pressure analog for the analysis of natural gas transportation networks*. Master Thesis. The Pennsylvania State University, State College, PA.
- Leong, Y. C. and Ayala, L. F. (2013). *A robust linear-pressure analog for the analysis of natural gas transportation networks*.
- Leong, Y. C. and Ayala, L. F. (2014). *Hybrid Approach by Use of Linear Analogs for Gas-Network Simulation With Multiple Components*.
- Menon, E. (2005). *Gas Pipeline Hydraulics*. Boca Raton: CRC Press Taylor and Francis Group.
- Mohitpour, M., Golshan, H., and Murray, A. (2007). *Pipeline Design and Construction*. New York: ASME Press.
- Osiadacz, A. J. (1987). *Simulation and Analysis of Gas Networks*. Houston: Gulf Publishing Company.
- Press, W. H., Teukolsky, S. A., Vetterling, W. T., and Flannery, B. P. (2002). *Numerical Recipes in C++: The Art of Scientific Computing*. Second Edition. New York: Cambridge University Press.
- US Energy Information Administration (2016). U.S. Natural Gas Pipeline Networks [Online image]. Retrieved January 28, 2016 from <https://www.eia.gov>
- US Energy Information Administration (2016). Heat Content of Natural Gas Consumed. Retrieved from <https://www.eia.gov>
- Valerus Company (2016). A compression station in Tapinhoa, Brazil [Online image]. Retrieved January 28, 2016 from <http://www.valerus.com/>
- Wu, S. (1998). *Steady-state simulation and fuel cost minimization of gas pipeline networks*. Ph.D Dissertation, University of Houston, TX.
- Wu, S., Rios-Mercado, R. Z., Boyd, E.A., and Scott, L.R. (2000). *Model relaxations for the fuel cost minimization of steady-state gas pipeline networks*. Math Comput Modell.
- Weymouth, T. R. (1912). *Problems in Natural Gas Engineering*. Transactions of ASME.

Wood, D., and Carl, O.A (1972). *Hydraulic Network Analysis Using Linear Theory*.  
Journal of the Hydraulics Division, ASCE.